TAMPEREEN TEKNILLINEN YLIOPISTO
TAMPERE UNIVERSITY OF TECHNOLOGY

HAMZAH MUKHTAR

LIGHT DRIVEN SURFACE PATTERING OF SUPRAMOLECULAR PHOTOACTIVE POLYMERS

Master of Science Thesis

Examiner: Prof. Arri Priimägi
Examiner and topic approved by the Faculty Council of the Faculty of Chemistry and Materials Science
on 01 February 2016

ABSTRACT

HAMZAH MUKHTAR: Light driven surface pattering of supramolecular photo-active polymers.
Tampere University of Technology
Master of Science Thesis, 50 pages
December 2018
Master's Degree Programme in Materials Science
Major: Polymers and Bio-materials
Examiner: Professor Arri Priimägi
Keywords: Azobenzene, Photoactive polymers, Supramolecular chemistry, Surface relief gratings, Photoisomerization, Hydrogen bonding and halogen bonding

Azobenzene containing photo-responsive polymers have gained much attraction due to their reversible photoisomerization and the different types of photoinduced phenomena that can be induced by the photoisomerization process. Photoinduced anisotropy, for instance, is of much interest for potential applications in optical/holographic data storage and optical switching. Photoinduced surface pattering, the topic of this work, is studied for applications in diffractive optics and microfabrication.

In this work the aim is to systematically study the effect of (i) azobenzene concentration, (ii) the molecular weight of the polymer where the azobenzene are incorporated into, and (iii) different types of non-covalent bonds through which the azobenzene molecules are attached to the polymer, on the formation of photoinduced surface relief gratings (SRGs). As the polymer matrix, poly(4-vinyl pyridine) (P4VP) was used. For (i) and (ii), 4-hydroxy-4′dimethylaminoazobenzene, that forms hydrogen bond with P4VP, was used. For (iii), three azobenzenes and two non-covalent interactions (hydrogen bond and halogen bond) were compared. The purpose here is to compare the non-covalent bonding effects on the efficiency of the SRG formations and to determine the most efficient non-covalent interaction for azobenzene containing polymers, especially in the low concentration regime.

For all of the three azobenzenes studied, the polymer molecular weight ranged from 1kD to 7kD and a series of samples was prepared with different azobenzene concentrations (1 mol% to 10 mol%). The samples were prepared with spin coating and the SRG formation was carried out via interference lithography, and the dynamics of the SRG formation in different complexes was studied through real time diffraction measurement of a probe beam during the inscription process.

The hydrogen bonded complexes showed an increase in the diffraction efficiency with an increase in the azobenzene concentration and it is observed that the azobenzene concentration and the polymer molecular weight are inversely proportional in terms of their effect on the efficiency. On the other hand, from the comparison of hydrogen and halogen bonding, it is evident that the halogen-bonded complexes surpass the hydrogen bonded-complexes and create more efficient gratings even at the lower concentrations, which is important for future optimization of non-covalently functionalized azobenzene containing polymers.

PREFACE

The research work reported in this diploma thesis was carried out at the Department of Chemistry and Bioengineering in Tampere University of Technology Finland, within the group SPM (Smart Photonic Materials) under the supervision of Professor Arri Priimägi. The work was funded by the Emil Aaltonen Foundation, who is gratefully acknowledged for their support.

I would like to express my deep gratitude to Professor Arri Priimägi for providing me with the opportunity to conduct my thesis work under his supervision. I am grateful to all my group mates for their guidance and directional assistance during the research work.

I want to thank all research group members for the supportive working environment in the laboratory and in office. I am highly grateful to Professor Arri Priimägi for the time he spent to teach me the tools to complete this diploma thesis work. During my thesis work I have been able to excel my skills and knowledge on photoactive polymers and the tools to study them.

Finally, I would like to acknowledge my family and friends for motivating me and supporting me during my whole study period and particularly my parents who have always been very supportive regarding my life goals.

Tampere (30-12-2018)

Hamzah Mukhtar

CONTENTS

Contents

LIST OF FIGURES AND TABLES

LIST OF SYMBOLS AND ABBREVIATIONS

Azo	Azobenzene
HB	Hydrogen Bonding
XB	Halogen Bonding
SRGs	Surface Relief Gratings
LC	Liquid Crystalline
T_g	Glass Transition Temperature
UV	Ultra Violet
GHS	Guest Host System
AFM	Atomic Force Microscopy
PIA	Photoinduced Anisotropy
TUT	Tampere university of Technology
σ-hole	Form of distribution/ Positive spot in halogen bonding
RPM	Rotation per minute / Rounds per minutes
Wt%	Weight percentage
Mol%	Mol percentage
Propanol	Iso-Propyl Alcohol
DMF	Dimethylformamide
$CHCl_3$	Chloroform
Milli-Q	Highly pure water
P4VP	Poly(4-Vinylpyridine)
4-Hydroxy	(E)-4((4-(dimethyl amino)phenyl)diazinyl)phenol
Azo-I	E)-N, N-dimethyl-4-((2,3,5,6-tetra-fluoro-4-iodo-phenyl) diazinyl) aniline
Azo-T	(E)-4-((4-(iodo-ethynyl-phenyl-diazinyl)-N, N dimethylaniline
Diff. Effi. %	Diffraction efficiency in percentage
H	Hydrogen Atom
λ_{max}	Maximum wavelength (of Absorption)

1. INTRODUCTION

Since the mid-20th century, azobenzene molecules and azobenzene containing polymers have been intensively studied. Azobenzene is an aromatic molecule, exhibiting efficient and reversible photoisomerization. The azobenzene molecules may modify their conformation between thermally stable *trans* and metastable *cis*-states upon a photon absorption. Large structural changes are caused by the isomerization reaction in azobenzene conformation which prominently affects its physical and spectroscopic properties (color, dipole moment, hardness anisotropy) [1] [2] [3]. Azobenzene is a prototype molecular switch used in many applications such as photo-responsive polymers, protein probes, photochemical systems, functional surfaces, holographic data storage devices and light controlled dug release [4] [5] [6] [7].

Photoisomerization is the phenomenon where azobenzene molecules undergo structural changes upon absorption of a photon and electronic excitation in the range of UV and visible electromagnetic spectrum. Light elicits the *trans-cis* isomerization within the absorption band of the *trans*-form, while reverse isomerization is carried out thermally or by light irradiation matching with the absorption spectrum of the *cis*-form [3]. The thermal reconversion rate is highly dependent on the substitution pattern of azobenzenes which can range from nano-second [8] to all the way up to several years [9]. Due to the wide span of thermal *cis*-lifetime, azobenzenes can be used for multitude of applications, some of which require bi-stable photo-switching (e.g. data storage) while others benefit from fast thermal reconversion (e.g. optical switching). A strong non-linear response is raised by substitution with electron donating and accepting groups, such azobenzenes are known as pseudo-stilbenes and they exhibit short *cis*-life and have a significant overlap between the *trans* and *cis*-forms spectra [3]. This enables that both *trans-cis* and *cis-trans* photoisomerization are driven by same wavelength, which causes the continuous cycling of the molecules between the two states and directs to acceleration and enhancement of many photoinduced effects [1] [3].

When azobenzenes are incorporated into polymers, one can induce photoinduced anisotropy (PIA), into the material upon irradiation with polarized light, which gives rise to many exciting optical phenomena. Such photoinduced anisotropy was observed in 1960s in azobenzene containing viscous liquids and polymers and was associated with photoisomerization reaction. The findings of photoinduced anisotropy phenomenon in viscous liquids containing azobenzene molecules have opened new horizons for the research and study of azobenzene and its derivatives. [10]. This phenomenon provides a useful tool for the creation of optical components, the combination of materials science and optics opens a great spectrum of opportunities. This introduces new solutions and

bring innovations to meet the growing industrial demands like diffractive optical elements, waveguiding and optical data storage etc. [11]. Different applications require different life times, as mentioned and PIA requires azobenzenes with shorter *cis*-life time [3].

The photoisomerization of azobenzenes triggers also other interesting phenomena. Amongst the most fascinating ones, in thin films photoisomerization can cause surface mass transport, resulting in the formation of surface relief gratings (SRGs). The SRG formation occurs efficiently in azobenzene containing amorphous polymers, when spin coated thin film is exposed to light interference pattern [3]. The gratings are erasable as the mass migration is reversible and erasure is conducted thermally or with light [2] [3] [12]. The grating formation on the surface of the film causes light diffraction and the diffraction efficiency depends on the quality of the SRG formation and SRGs also require the azobenzene molecules with short *cis*-life time [3].

The SRG formation was initially observed in 1995, in polymers into which the azobenzenes were covalently bonded [13] [14]. The difficult preparation and multistep synthesis of such covalently functionalized systems made them time consuming and expensive to prepare. Therefore 12 years later systems with spontaneous and non-covalent interactions between the polymer and the azobenzene molecules were introduced for SRG formation [15]. Later research works revealed that the SRG formation phenomenon can be observed in many non-covalent systems, including ionically bonded, hydrogen bonded (HB) and halogen bonded (XB) [16] azobenzene-containing polymer complexes [2] [3].

These non-covalent bonds eliminate the necessity of synthesis for functionalized polymers and make the process simple to mixing of compounds in required ratios [2]. The ratio between polymer and the chromophore affects the properties of the complex. The higher chromophore ratio causes chromophore aggregation which affects the material performance and typically decreases the optical response as well [3]. The hydrogen bonding and halogen bonding opened new windows and opportunities with the ease of conventional guest host systems between the polymer and azobenzene to prepare efficient photo-responsive azopolymer complexes [17]. This methodology has made the sample preparation much faster, easier and cheaper. This ease of sample preparation opens up space to study in detail the influence of azobenzene chromophore concentration and polymer molecular weight on the SRG formation and performance. SRG formation is still not fully understood phenomenon and requires more research work for concrete findings to fully understand the phenomenon. This study work will be focusing to study the SRG formation at low concentration limits with different molecular weights of polymer.

The current study is focusing on different aspects of the supramolecular functionalization and we employ to establish a correlation between the dye concentration and the

polymer weights and type of bonding in polymer-dye complexes. This includes the study of hydrogen and halogen-bonded complexes created from three different azobenzene chromophores and one amorphous polymer with different molecular weights. The first aim is to identify the lowest concentration of azobenzene chromophores in polymer which still allows the mass-transport and the formation of SRGs to occur when keeping the polymer weight constant. The second aim is to study the effect of the polymer molecular weight on the SRG formation by keeping the azobenzene concentration constant. The third aim is to compare the effect of two non-covalent interactions (halogen bonding and Hydrogen bonding) on the mass transport efficiency.

The experimental work was carried out in the Laboratory of Chemisry and Bioengineering at TUT. It consisted sample fabrication via spin coating, characterization via profilometry and absorption spectroscopy, SRG formation via laser interference lithography, and real-time diffraction experiments. The results of the Thesis work guide towards optimization of non-covalent SRG-forming photo-responsive polymers, especially for applications where low azobenzene concentration is beneficial.

2. AZOBENZENES

Azobenzene (or azo in an abbreviated form) is an aromatic molecule where an azo-bridge (-N=N-) links together two phenyl rings as shown in Figure 2.1. Azobenzene and its derivatives are photosensitive and well known for their ability to photo-isomerize when irradiated with light of proper wavelength [3]. The name azo is derived from the French word for nitrogen, azote. Azo-containing polymers have gained much consideration during last few decades and have depicted a huge potential in the research work. The azobenzene chromophores being chemically stable have encouraged their study as dyes and pigments. Azobenzenes have been used as commercial pigments and colourants in textile industry, and even today, around 70% of commercial pigments are azo-based [4] [18].

2.1 Azo-Chromophores

Azobenzenes can be classified into three types, known as azobenzene-type, amino-azobenzene type and pseudo-stilbene type molecules as shown in Figure 2.1. Azobenzenes are classified into these types base on relative energies of $n \rightarrow \pi^*$ and $\pi \rightarrow \pi^*$ transition [3]. The tailoring of azobenzene molecules relies on π-electron structural delocalization in which changes depending on substituents.

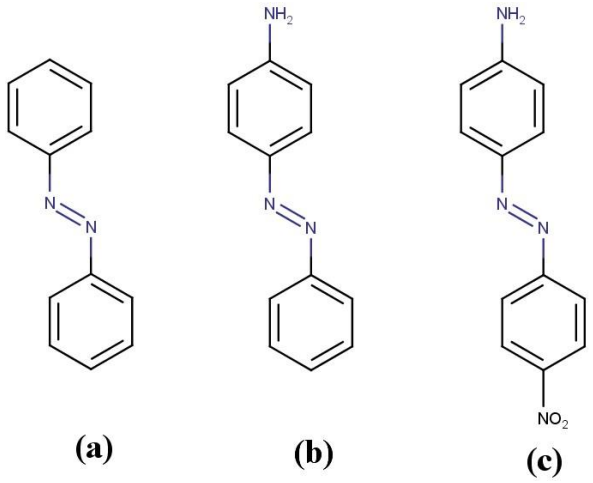

Figure 2.1: *Azo-derivatives termed as (a) azobenzenes, (b) amino-azobenzenes, (c) pseudo-stilbenes*

The strong absorption is observed in azobenzene molecules in the wavelength range of 300 to 600 nm. They exhibit yellow (azobenzene-type), orange (aminoazobenzene-type) and red (pseudostilbene-type) colours respectively resulting from their specific absorp-

tion spectra [4]. The azobenzene types (Figure 2.1) and their corresponding absorption spectra are shown in Figure 2.2. The azobenzene type molecules, in UV region, exhibit an intense $\pi \rightarrow \pi^*$ and at 440 nm a weak $n \rightarrow \pi^*$ band. The $\pi \rightarrow \pi^*$ band is red shifted for amino-azobenzenes (denoted as NHA in Figure 2.2) to the proximity of the $n \rightarrow \pi^*$ band, which is insensitive to substituent effects [3]. The third spectroscopic class, the pseudo-stilbenes (DR1 in Figure 2.2) are substituted with strong electron donor and electron acceptor groups. The $\pi \rightarrow \pi^*$ band is considered to be of lowest energy and the $n \rightarrow \pi^*$ is overshadowed by this intense transition for this substitution pattern, often referred as push-pull molecules [19]. Pseudo-stilbenes are sensitive to the local environment and in condensed phases, are also sensitive to packing and aggregation, which can be useful in some applications but detrimental for most. The $\pi \rightarrow \pi$ stacking escalates shifting of absorption spectrum [4]. Parallel or head to head aligned azo-dipoles are called J-aggregates and head to tail aligned azo-dipoles are called H-aggregates, respectively they give rise to redshift and blue-shift of the spectrum [4].

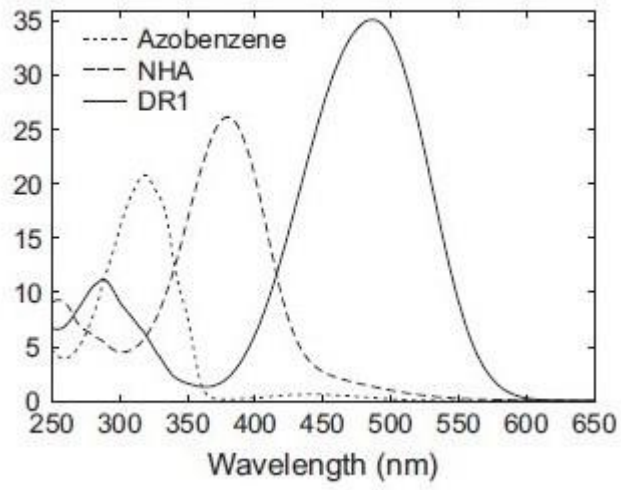

Figure 2.2: *Azobenzene's absorption spectra. Figure adopted from [3]*

The strong absorption also triggers photoisomerization process in the azobenzenes. The captivating properties of azobenzene and its derivatives, which are available now in a broad range of materials, are triggered by the effective and reversible *cis-trans* photo-isomerization phenomenon as shown in Figure 2.4 [18]. Photo-isomerization incorporates significant changes to the azobenzene molecules such as change of dipole moment and molecular shape. Azobenzene's thermally stable *trans* and metastable *cis*-states give it a unique ability to interconvert between these states with a photon absorption [5]. The dipole moment of 3.0 D is only exhibited by the *cis*-isomer and no dipole moment in *trans*-isomer. The azobenzene containing polymers exhibit non-linear optical properties, light induced dichroism and birefringence [6].

Reversible photoisomerization from *trans* to *cis* can be observed for many azobenzenes upon the exposure to a wide absorption band. As per the substitution pattern timescale, the azo molecule will thermally relax back to *trans* state depending on the irradiation wavelength and temperature [4] [6]. The azobenzene compounds experience significant changes in their absorption spectrum caused by photoisomerization, as shown in Figure 2.3.

Photoisomerization indicates that photon exposure can lead the molecule to change its geometry. The photoisomerization of azobenzenes and its complexes is fully reversible between two states, the thermally stable *trans* form and the metastable *cis* form as shown in Figure 2.4. It is considered one of the cleanest photoreactions observed, without any side reactions [18] [4]. Reconversion of isomerization can either be light induced or thermal, the rate of thermal reconversion intensively depends on azobenzene substitution pattern.

The *cis*-lifetime of all three classes are in the sequence of hours, minutes, and seconds respectively for azobenzenes, amino-azobenzenes and pseudo-stilbenes [3]. A rapid thermal isomerization reaction takes place for amino-azobenzenes and pseudo-stilbenes comparative to azobenzenes and *cis*-form spectra is only being projected through extrapolation techniques [3]. The pseudo-stilbenes have high dipole moment due to electron donors and electron acceptors added to the molecule.

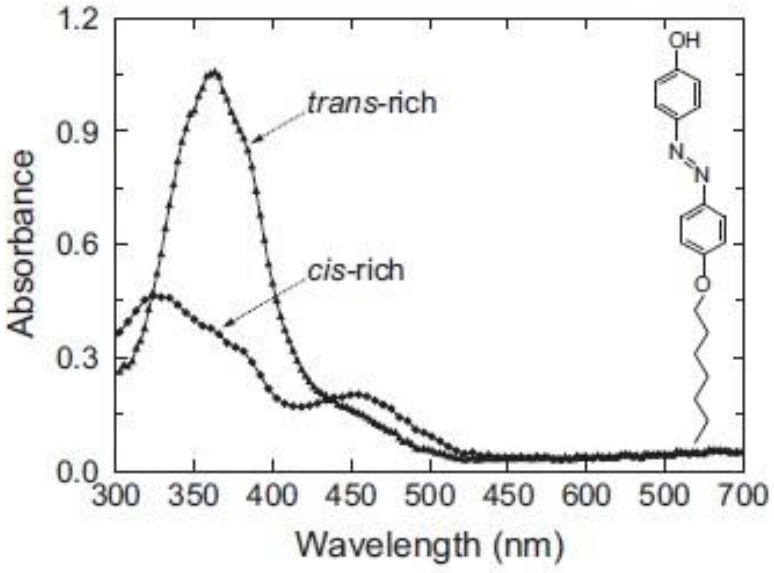

Figure 2.3: *Absorption Spectra of the trans-rich and cis-rich photo-stationary state. Figure adopted from [3]*

Through absorption spectroscopy (Figure 2.3), inherent photochromic (color change upon light absorption) nature of azo compounds offers a procedure to easily observe the isomerization kinetics and steady state composition. The photo-stationary state, i.e., the ratio between *trans* and *cis*-iomers under constant irradiation, is dependent on the quantum yield of the two isomerization processes for *trans* and *cis*-isomers of an azobenzene-containing sample. It is also dependent on relaxation rate being extremely sensitive to the local environment and irradiation conditions [3] [4]. The photo-stationary state is strongly dependent on wavelength, metastable *cis*-form inclines to more stable *trans*-form in a fixed timespan upon irradiation termination, which is determined by the chemical structure and local environment of the molecule [3].

Azobenzene type molecules are same like unsubstituted azobenzenes, the *trans-cis* isomerization is dependent on their transition from a bonding p-orbital to an antibonding p-orbital ($\pi \rightarrow \pi^*$ transition), positions in the UV region, and *cis-trans* isomerization depends on the transformation from non-bonding orbital to antibonding p-orbital ($n \rightarrow \pi^*$ transition), positions in the visible region of the spectra. An amino-azobenzene type molecule is formed by substitution of electron donating amino group ($-NH_2$) azobenzene which influences the $\pi \rightarrow \pi^*$ transition band to move closer to the $n \rightarrow \pi^*$ transition band in the visible region. Both acceptor and donor substitutions exist in pseudo-stilbene class which at blue-green wavelengths leads the absorption spectra to overlap for *trans* and *cis* states [4].

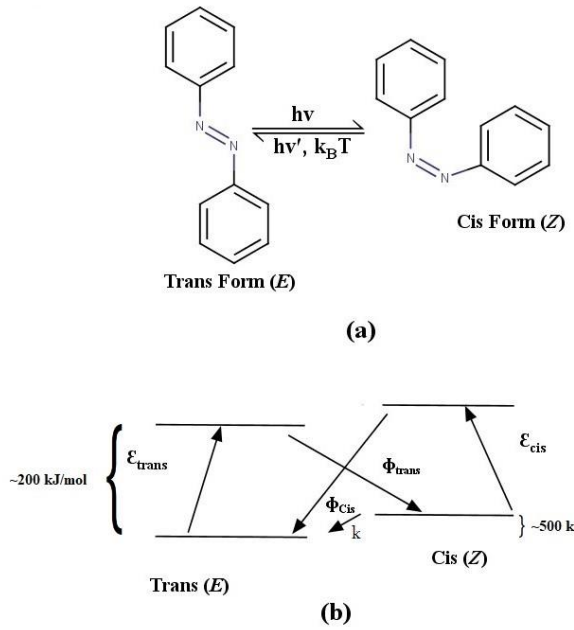

Figure 2.4: *(a)Azobenzene transformation between trans and cis state photochemically and relaxation (k) to the more stable trans-state thermally (b) Simplified state model for plain azobenzene. The trans and cis extinction coefficients are denoted by $\mathcal{E}_{trans}$ and $\mathcal{E}_{cis}$ ϕ refer to the quantum yield of photoisomerization and γ is thermal relaxation rate constant [3] [4]. ϕ_{Cis}. Figure adopted from [4]*

For plain azobenzenes, the transition state energies are shown in Figure 2.4 (b). The isomerization occurs in very small-time laps like in picoseconds and is inert to side reactions. The photostationary state can be attained during irradiation by the azobenzene-containing systems either in a bulky sample or in a solution where azobenzene chromophores are in the polymer matrix [3] [4]. In the glassy state of polymers, *cis*-isomers are lower in content in the photostationary state than in solution due to the rigid environment to allow for efficient photoisomerization [3]. Above the glass transitions temperature (T_g) of polymers or in solutions the, thermal *cis-trans* isomerization obeys the monoexponential (first order) relaxation kinetics. In glassy state non-uniform distribution of the free volume leads towards the higher rate of isomerization for a fraction of the molecule due to two exponential process [7]. Use of azobenzenes as the site-specific probe is the effect of the higher sensitivity of the isomerization kinetics to local environments to study the cross-linking behaviour of polymer and to determine the free volume distribution [3] [20].

The photoisomerization process is supposed to occur in two different ways, one is called inversion and other is called rotation mechanism, with a semi-linear and hybridized transition state, through one of the nitrogen nuclei the inversion takes place keeping the π-bond intact and the other takes place around the N=N bond by rotation rupturing the π-bond [4] [21]. Both methods bring the same molecular changes, with different isomerization processes where rotation mechanism demands more energy than the inversion isomerization, and for azobenzene isomerization, rotation mechanism demands higher free volume than the inversion mechanism [21]. Following Figure 2.5 illustrate the both rotation and inversion mechanisms,

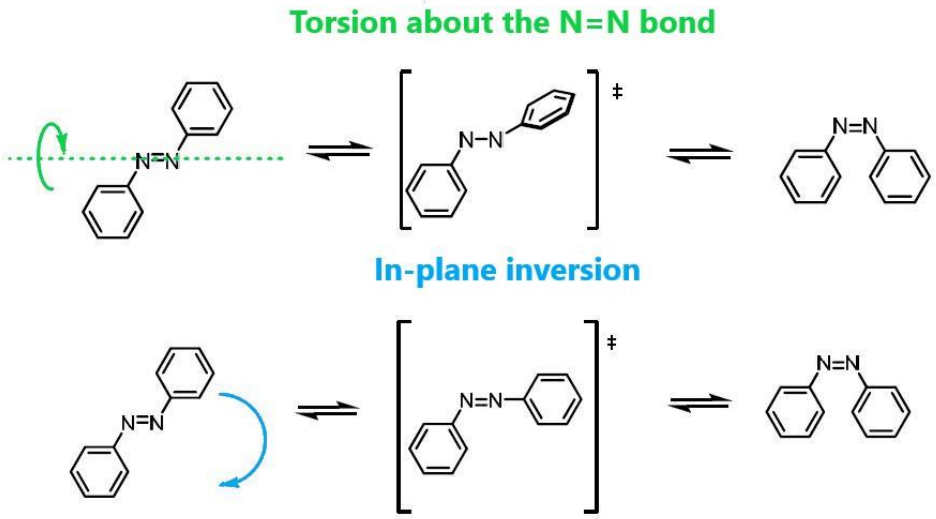

Figure 2.5: *The Isomerization mechanism of Azobenzenes [4] [22], Figure adopted from [22]*

Different chromophores and matrices support different mechanism and the mechanism that dominates strongly depends on the specific chromophore type and environment. The inversion mechanism is stated as the dominant one for most of the azobenzenes, due to its low free volume requirements which allows it to isomerize in materials like non-amorphous polymers [4].

The photoisomerization reaction of azobenzenes can be used to convert the light energy into mechanical energy by making reversible shape and volume changes in the material system. The strength of light induced mechanical forces can be compared to the contraction force of human muscle which can lead to possible application like artificial muscles or photo driven robotic devices [3].

2.2 Azo-Polymer Complexes

The light-induced processes triggered by the photoisomerization of the azobenzenes have been studied in different environments. The study work has been conducted in monolayers, vacuum evaporated thin films, hybrid organic-inorganic composites and polymeric materials. The azobenzene containing organic polymeric materials have various optoelectronic applications. The applications include light frequency conversion, optical data storage, waveguiding and optical signal processing, influenced by their easy availability, process-ability, low price and durability [19].

The incorporation of azo chromophores to organic polymers provides control to tailor the material properties by adjusting the concentration ratios of the elements [23]. The dye and polymer concentration determine the reactivity of the system and the application of the azo-containing polymers are based on photochromic, fluorescent, photorefractive, or nonlinear optical effects and develop the high response to optical fields of the active molecules [23]. The systems where higher concentration of the dye is used in the host polymer, it is essential to avoid the aggregation which can increase the scattering losses and can reduce the overall system response. Polymer doping with azo-dye can be carried out in different ways. The simplest way is that the guest dye is introduced to the host polymer (Figure 2.6 a) through simply dissolving it and in such guest-host systems no prominent intermolecular interactions are observed between the active dye molecules and the polymers [23] [24]. This easy incorporation with no interaction between the dye molecules and host polymer leads towards dye aggregation, which causes a reduction in glass transition temperature (T_g), limits, doping levels, affects thermal stability and crystallizes the polymer.

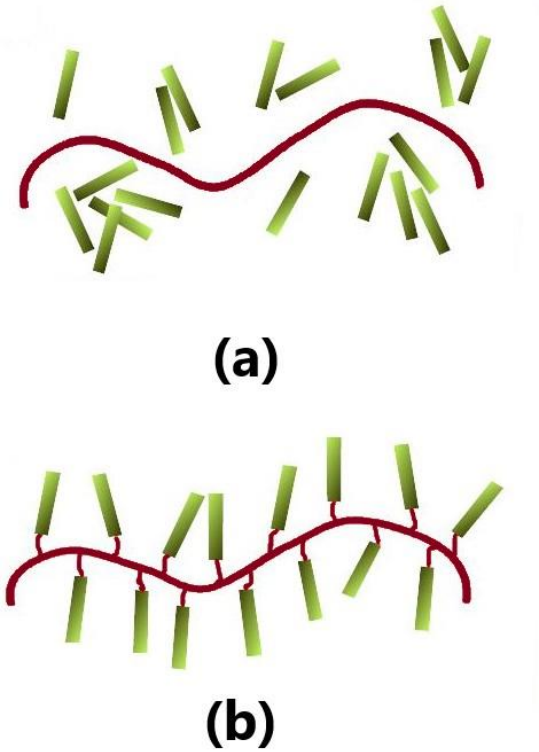

Figure 2.6: *Schematic illustration of (a) conventional guest-host system with no interaction between the guest molecule and host polymer (b) covalently functionalized side chain polymer [3]. Figure adopted from [3]*

The aggregation problem of the dye guest-polymer host system can be tailored by linking the active dye molecules covalently to the polymer backbone (Figure 2.6 b) or chemically making them as part of the polymer main chain itself. These systems provide higher doping concentrations without phase separation but with the reduced thermal relaxation of molecular alignment. However, such covalently-functionalized systems need complex organic synthesis for each dye-polymer combination which makes them less attractive and expensive than guest-host systems [23] [24]. The covalently functionalized polymers show higher optical response and lower optical losses comparative to guest-host systems. The covalent attachment obstructs the chromophores orientational relaxation and has higher glass transition temperature than the guest-host system. In applications that require net alignment of chromophores, this leads to higher temporal and thermal stabilities. Proper selection of host polymer can reduce the aggregation by resulting enhanced intermolecular forces between dye molecules and the polymer [3] [23].

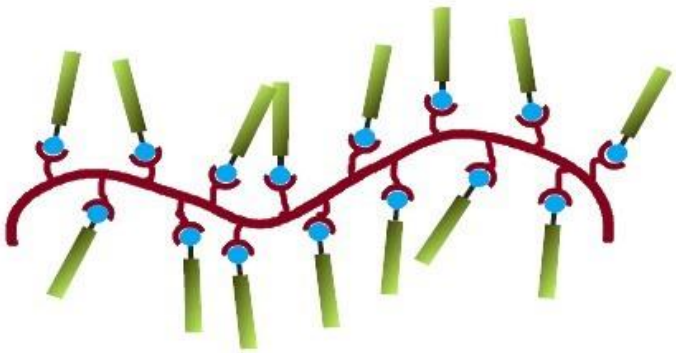

Figure 2.7: *Guest host (GH) system with intermolecular interactions between polymer host and Guest Chromophore to prevent their aggregation [3] Figure adopted from [3]*

The non-covalent interactions formation is spontaneous, opposite to the synthesis strategies based on covalent bonding and hence provides advantages compared to covalently functionalized polymers. In such systems, the side chain concentration can be tuned over a broad range without laborious organic synthesis, up to the point where each repeat unit of the polymer is engaged, if the polymer and the side chains have complementary recognition motifs [3]. Further, with two or more side chains the polymer can be functionalized, each chain possessing a particular role in the material system. For the regular guest-host systems, such modular tunability can be realized without sacrificing the ease of preparation. Polymer-dye complexes, the non-covalently functionalized optical materials can be anticipated as advantageous they combine the benefit of guest-host system (Figure 2.7) and the covalently functionalized polymers [3].

Supramolecular side chain polymers consist of a polymeric backbone with non-covalently bonded side chains. This can be carried out with different types of interactions including ionic interaction, metal coordination, single and multiple hydrogen bonding or combination of these interactions [3]. The largely used non-covalent bonding for azo-polymer complexes is hydrogen bonding (HB). HB is deeply understood and largely used in materials science and has provided solid and encouraging results and has led to the supramolecular concept to a solid place in the azobenzene study as photoactive materials [2]. Hydrogen bonding provides easy access to manipulate the polymer-chromophore complexes and is easy to manage compared to ionic bonds which are more environment sensitive [25]. Photoinduced anisotropy can be improved in guest-host polymers by the introduction of hydrogen bonding between host-dye in guest-polymer [26]. Another noncovalent interaction called halogen bonding (XB), which is newly adopted tool for the study of supramolecular chemistry. Several examples of azobenzenes involving halogen bonded supramolecular structures have recently been reported [27].

2.3 Photoorientation / Photoalignment

The orientation mechanism of azobenzene chromophore by polarized light is termed as photo-orientation, which is has been thoroughly studied for many years for azobenzenes. The capability of some materials to become optically anisotropic upon irradiation with polarized light in photographic silver emulsions has been known since the beginning of 1900s. This phenomenon was observed in azobenzene containing viscous liquids and polymers in 1960s and was later related with photoisomerization reaction [3] [4] [28] [29]. The polarization component of the incident light parallel to the dipole moment of chromophore's transition causes the excitation and the photoisomerization [1]. Azobenzenes along their transition dipole axis absorb polarized light and the absorption probability relies on the angle (ϕ) between azo dipole axis and the light polarization, the angle value changes as $Cos^2\ \phi$.

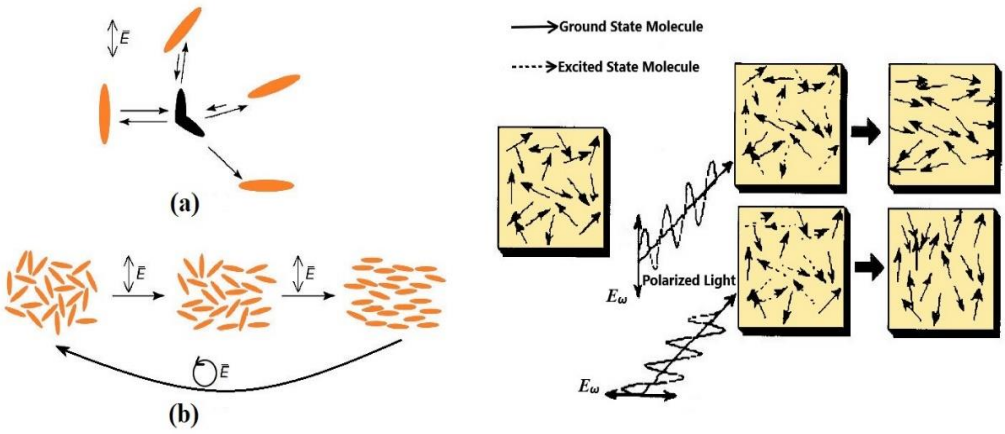

Figure 2.8: *Photo-orientation of azo-molecules, (a) The molecules are aligned along the incident light polarization direction, isomerize, and reorient and the ones aligned perpendicular cannot absorb and remain stationary. (b) irradiation of isotropic samples which directs to the accumulation of chromophores in the perpendicular direction and circular light polarization restores isotropy [30]. Figure adopted from [4] [30]*

Azobenzene molecules experience strong photon absorption when their transition dipole moment or molecular axis is parallel to the incident light polarization direction and the molecules perpendicular to the polarization of light remain fixed and do not isomerize or reorient [4] [31] [32]. This causes a simultaneous increase in the chromophore population perpendicularly aligned and chromophores aligned with the light polarization experience a net depletion [4]. When exposed to the irradiation light, for an initially isotropic angular distribution of azo-molecules, many of them will absorb the light and move to *cis*-form and then reorient back to *trans* form with a new random direction, which eventually brings more chromophores perpendicular to the polarization of light

[4]. The orientation caused by the polarized light is reversible and can be changed by new irradiating light polarization [4]. Circular polarization or unpolarized light is used to change the angular distribution of the chromophores and orients them randomly [30]. The light polarization, a contactless method, provides the freedom of controllability over light intensity, polarization direction, wavelength and manipulation of interference patterns [33].

The photoisomerization reaction empowers one to reorient the chromophores with linearly polarized light, escalating birefringence, dichroism, and in particular conditions, to nonlinear optical response in the material system [3]. The incorporation of azo-chromophores into polymer matrix makes the molecules stable and by inducing anisotropy in the azo-polymer system, the statistical reorientation can be very rapid which makes the material strongly birefringent leading to the possibility of applications in photonics (optical switching, laser beam modulation) or optical/holographic data storage [4].

2.4 Photoinduced Birefringence

Optically anisotropic materials with properties dependent on the light beam direction, are called birefringent. Birefringence arises by the molecular bond strengths and anisotropic crystal arrangements [34]. In all birefringent materials at least along one axis the light can travel without any disturbance to any of its component of its electric vector (uniaxial materials), it is called the optic axis, some materials have two of them (biaxial materials). Optics axis (Figure 2.9) is considered as the reference axis. The light travelling in any other direction through the birefringent material faces two different refractive indices (i.e., different light propagation speed in the material) and rips in to components that have perpendicular polarization and travel at varying speeds [34]. The component polarized perpendicular to the optic axis encounters the ordinary refractive index (n_o) when the light travelling perpendicular to the optic axis (red ray) and the component parallel polarized to the optic axis encounters the extraordinary refractive index (n_e). Light entering a birefringent material at an oblique angle causes a component to encounter ordinary refractive index (n_o) vibrating in the plane perpendicular to the optic axis [34].

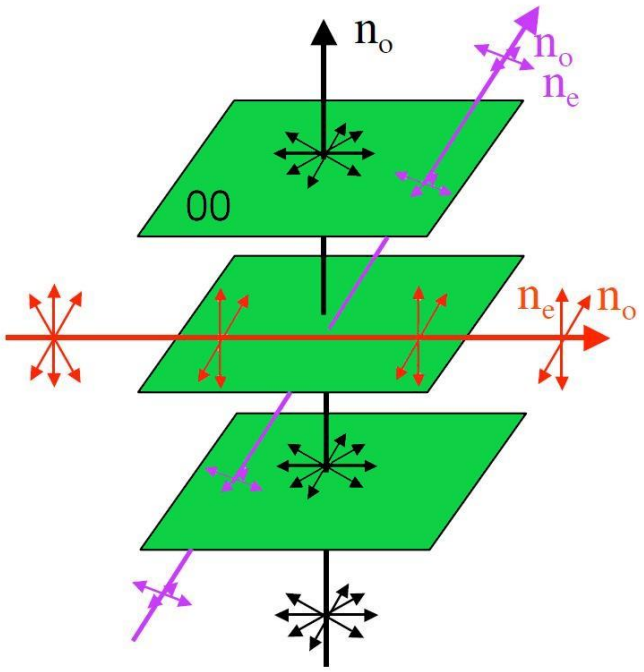

Figure 2.9: *Optic Axis (Black Ray), Light perpendicular to Optic Axis (Red Ray), Light entering at oblique angle (Purple Ray) [34]*

Photoinduced birefringence, resultant of statistical reorientation in azo-containing polymers, means light induced anisotropy in the refractive index of the material for the ordinary and extraordinary waves, which is stated as $\Delta n = n_e - n_o$, where n_e and n_o are refractive indices (Figure 2.9) [4] [35]. Depending on the speed propagation of ordinary or extraordinary wave, the material is positively or negatively birefringent [36]. Circularly polarized light irradiation enables to restore the in-plane isotropic state ($n_e = n_o$) and heating above T_g can attain fully isotropic state [4] [36]. The dichroism depicts the anisotropy of the absorption coefficient of the material with respect to polarization of the incident beam. The polarization of the incident light provides controllability over the orientation direction and the direction of the reference axis.

Azobenzene groups facilitate the mesogen-like cooperative motions even for amorphous samples below T_g, which makes the photoinduced birefringence phenomenon sometimes very efficient [4]. For any induced orientation good temporal stability is exhibited by relatively high T_g amorphous polymer, preventing thermally induced relaxation of the azobenzenes from the anisotropic towards the isotropic state. Heating causes disorder and full isotropy can be attained upon heating above T_g [4]. A short void between the polymer and the chromophores decelerates the growth of birefringence but still promotes stability, owing to stalled motion [4]. Astonishingly high levels of birefringence can be attained by the main chain azos, depicting relatively high polymer movement.

The orientation direction can be controlled by the incident beam polarization and the manipulation of incident beam makes it possible to create diffraction gratings based on

the local changes in the material birefringence [35]. The first azobenzene containing amorphous polymer with a birefringence grating on it was reported by Todorov *et al*. in 1984 and later on, birefringence values up to 0.5 have been achieved in the azobenzene containing polymer systems [31] [35]. Before the formation of surface relief grating was observed in 1995 [13], birefringence was considered the only factor for diffraction properties of azopolymer gratings [13]. The technologically great achievement could be a rewriteable optical memory system development based on azobenzene holography and also tunable waveplates and optical switches, due to fact that the birefringence can be induced and erased hundreds of thousands of times, have been intensively studied [4] [36].

2.5 Surface Relief Gratings (SRGs) / Mass Transport

In 1995, in azobenzene containing polymer films, a large-scale surface mass transport was reported after ten years of the discovery of reversible birefringence gratings. Since then surface relief formation has activated a large scale of both fundamental and applied research [13] [37]. The surface deformation according to interference pattern was observed in films as they were irradiated by the light interference pattern. The spin cast sample, a pseudostilbene side chain azopolymer film from Poly-Disperse Red-1 acrylate, a classical SRG-forming polymer, were introduced in the work by Rochon *et al*. [13] [37]. The SRG phenomenon can occur even 100 ^{o}C below the glass transition temperature of the polymer and allows the formation of micron-scale surface patterns. This makes it interesting to understand how light can produce macroscopic movements of polymeric materials well below the glass transition temperature of the polymer [37].

Formation of the photoinduced surface relief gratings, in azobenzene containing amorphous polymers in the glassy state, is among the most surprising physical process. Large-scale mass migration of the polymer chains can be caused by the photoisomerization of the nanometer-sized chromophores over distances of several microns. The free surface of the film deforms as a resultant of the irradiation light field and reproduces the intensity or polarization variation as a surface relief grating upon exposure to the interference pattern of irradiation light with spatial changes of the intensity or polarization. This opens a new window for the production of diffractive optical and photonic devices as this method provides the opportunity to inscribe highly elaborate surface structures with hundreds of nanometers of modulation depth. The inscribed surface structures can be erased thermally or with light [3]. The surface patterning can be achieved with irradiation intensities of only 5 mW/cm^2 as it occurs in a wide range of azobenzene containing materials systems [3]. The nature of the material system and experimental arrangement details put a large effect on the efficiency of the process making it a complex and dependent on several varying parameters [3] [38].

A strong bonding is necessary between chromophores and the polymer chains for effective photoinduced mass migration in azo-containing polymer systems, consequently in

conventional guest host type polymer systems, very weak surface relief gratings can be inscribed [3]. Polarization of the inscribed beam is highly responsible for the efficiency of the surface relief gratings formation [3]. This phenomena behind this photomechanical process is not yet completely understood even after massive research and practical work [38]. Different models have been projected but none of them provides complete understanding over the experimental observations. The photoinduced SRG formation in the azo-containing polymer systems seems to be triggered by several microscopic mechanisms whose comparative significance is dependent on the material system [38]. Such as, there are some fundamental differences in the formation of SRGs in liquid crystalline and amorphous polymers, in liquid crystalline polymers the migration of molecules into the irradiated region is observed while in amorphous polymers the dark regions of the intensity distribution face concurrence with the with maxima of the surface pattern [3].

Atomic-force microscopy images of the SRG structures obtained under interference irradiation show a sinusoidal curve pattern (Figure 2.10) with particular values of fringe spacing and modulation depth depending on the experimental setup, while the modulation depth of the grating is highly material-dependent [33] [38].

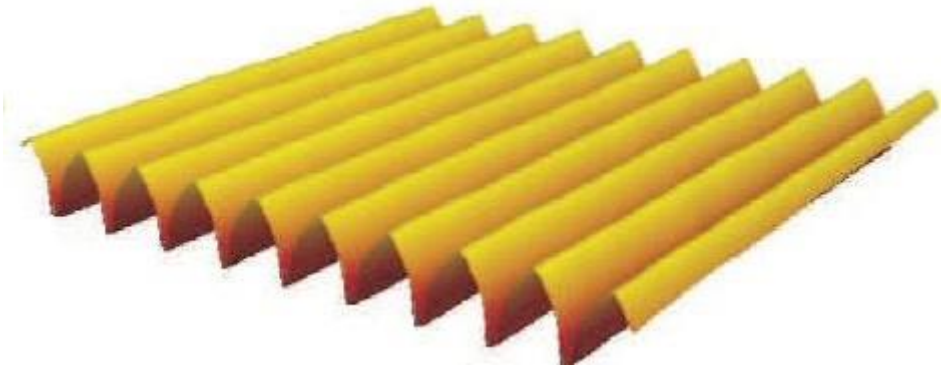

Figure 2.10: *Surface Relief Grating the Sinusoidal Curve Pattern with particular modulation depth and fringe spacing [38]*

For azobenzene containing polymers the mass transport process is a highly complex cascade of events that derives from molecular-scale photoisomerization. The experimental parameters and the material itself define the driving mechanism and this is still under debate to define a universal theory [18]. The effect of polymer structure on the SRG efficiency has not been established yet although the molecular weight of polymer and glass transitions are well known parameters as well as the content of the azobenzene in the material [18]. The azobenzene chromophore concentration effects are very interesting as it can lead to understand the magnitude of power the azobenzene photoisomerization reaction can actually translate into big macroscopic movements [18].

The dependence on the dye concentration of the mass transport has been studied in several systems from medium to high concentrations of azobenzene. For higher values of

azobenzene chromophore concentration like above 75 mol% the intermolecular interactions between adjacent chromophores occurs which causes reduction in SRG formation efficiency [18]. Herein, we study the hydrogen and halogen-bonded polymer-azobenzene complexes by systematically increasing the dye concentration and also the polymer molecular weight to study and analyze their effect on SRG formation especially in the low concentration regime.

3. NON-COVALENT BONDING

The chemical bond between two atoms, is divided into two types, covalent and non-covalent bonding. Both bonding types differ in their strengths as the sharing of an electron pair between two atoms causes covalent bonding, which is stronger compared to non-covalent interactions. Generally, a stronger bond is rated as primary bond and a weaker bond is rated as secondary bond. As per the strength, the covalent bonds are described as the primary bonds and non-covalent interactions as the secondary bonds [39].

A non-covalent bond differentiates itself from covalent bonding as it involves more disperse variations of electromagnetic interactions between molecules or within a molecule. Unlike covalent bonding, it does not involve the electrons pair sharing. The energy released in the formation of the non-covalent bonds is on the order of 1-5 kcal/mol, i.e., comparatively very small to covalent bonding which has the energy of the order 100-200 kcal/mol [39]. It is because of the low average kinetic energy at room temperature that is about 0.6 kcal/mol that non-covalent complexes can be stable, yet dynamic, and hence continuously break and reform [39]. At physiological temperatures (25 – 37 ˚C) in spite of that the non-covalent interactions are weak and have transient existence, various non-covalent bonds often act together to produce exceedingly stable and explicit associations between different parts of a large molecule or between various macromolecules [39]. Non-covalent interactions mediate recognition of complementary molecular moieties by driving spontaneous folding of proteins and nucleic acids. In biological systems, non-covalent interactions command the conformation and interaction. In supramolecular chemistry non-covalent interactions are the dominant type of interaction [40].

Non-covalent interactions result from number of different forces and are generally categorized into four types as following [40]

1- Electrostatic interactions
    - Ionic interactions
    - Hydrogen bonding
    - Halogen bonding
2- Van der Waals forces
3- π-effects
4- Hydrophobic effect

Hydrogen and halogen bonds are two highly studied non-covalent intermolecular interactions. HB is a particular type of dipole-dipole interaction (Figure 3.1). In such type of

interaction, the neighboring molecules arrange themselves in such an array that the positive pole of one molecule is close to the negative pole of the other molecule. The comparison of the intermolecular forces states that they are weaker relative to ordinary covalent bonds but when compared to each other, the hydrogen bonding is the strongest [41] [42].

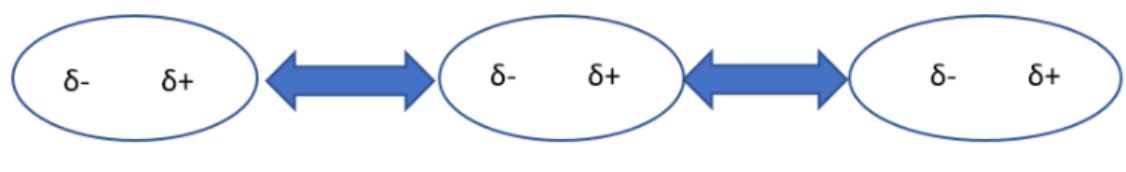

Figure 3.1: *Intermolecular Interactions: Dipole Forces*

In this study we study only hydrogen and halogen bonding based azobenzene containing systems and other type of non-covalent interactions are not of much interest in this study.

3.1 Hydrogen Bonding

Hydrogen bonding can be defined as per IUPAC: "The hydrogen bond is an attractive interaction between a hydrogen atom from a molecular or a molecular fragment D — H in which D is more electronegative than H, and an atom or group of atoms in the same if a different molecule, in which there is evidence of bond formation [43]"

Hydrogen bonding was discovered in the beginning of 20th century and human DNA and water (H_2O) is one of its famous examples. The hydrogen bonding phenomena and with acceptor-donor concept has already been vastly studied in supramolecular photoactive polymer interactions. Priimägi *et al* [38] studied it and published detailed research work on hydrogen bonding between chromophore and polymers which defines the phenomena with different types of dyes and molecular weights and their behavior against SRGs inscription and their efficiency with respect to weight and ratio of the dyes and the polymers [17] [38].

Hydrogen bonding is a non-covalent interaction between an electronegative atom (generally O, N, F) and a hydrogen atom covalently bonded to another electronegative atom. Generally, a hydrogen atom makes a covalent bond with only one other atom. The HB is relatively stronger than other intermolecular interactions since the small size of hydrogen atom makes it vulnerably good in donating and electronegative atoms are efficient in attracting them. It is depicted as the hydrogen (H) atom covalently bonded to the electronegative atom D and another electronegative atom A, illustrated as D — H---A, here D — H is stated as the hydrogen bond donor and ---A as the acceptor. The large difference in electronegativities occurs between H and the N, F, O atoms in molecules containing N-H, O-H or F-H bonds. It causes the H atom to contain large partial

positive charge and electronegative atoms contain large partial negative charge [44]. In induction of the HB the electronegativity is considered the major player, but the steric effects also play an important part in the formation of the bond [44]. The HB in the beginning was schemed as between a highly electronegative atom bonded to hydrogen forming bonding with another electronegative atom.

$$^{-\delta}N—H^{\delta+} \qquad ^{-\delta}O—H^{\delta+} \qquad ^{-\delta}F—H^{\delta+}$$

$$D — H \text{ ---- } A$$

Where D = N, F, O, etc. and A = another electronegative atom.

The above scheme is presented as acceptor and donor, where D must be electronegative and D — H is the covalently bonded donor and bond is polar and A is the acceptor. Both donors and acceptors are generally nitrogen or oxygen atoms in biological systems especially those atoms in amino (—NH_2) and hydroxyl (—OH) groups [39]. All the covalent bonds (O — H and N — H) bonds are polar and HB can be formed by their H atoms. Conversely C — H bonds are non-polar indicating their H atoms are almost not involved at all in hydrogen bonding [39]. The interesting feature of hydrogen bonding is that under relatively moderate conditions the bonding can be switched reversibly (Figure 3.2) by heating or other physical stimuli [45].

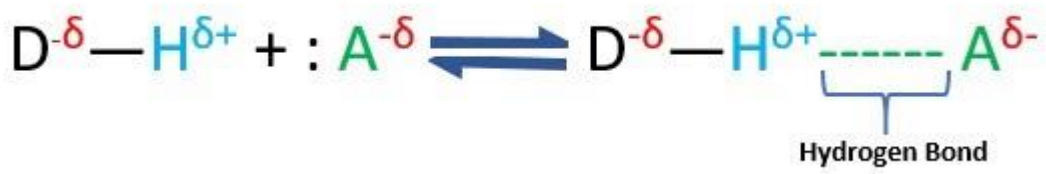

Figure 3.2: *HB reversible acceptor-donor illustration*

Water molecules are considered the best example of hydrogen bonding as it incorporates unique properties to water molecules which keep water in liquid form and provide it high boiling temperature [42]. The hydrogen atom in one water molecules is attracted to a pair of electrons in the outer shell of an oxygen atom in an adjacent molecule.

Directionality is an important feature of all the HB. The hydrogen atom, the donor and the acceptor atom, all lie in a straight line in the strongest hydrogen bonds. The D — H---Y angle is usually linear (180̊) and the angle more near to 180 the hydrogen bond is more strong and shorter is the H---Y distance. The hydrogen bond formation causes an increase in the length of the D — H bond. The larger the length of D — H bond in D — H---Y the stronger is the H---Y bond, because the acceptor pulls the hydrogen away

strongly from the donor [43]. Mostly, hydrogen bonds are 0.26 to 0.31 nm in length almost twice the covalent bonds length between the same atoms [39].

3.2 Halogen Bonding

Halogen Bonding (XB) is also a noncovalent interaction, it is defined as per IUPAC: "A halogen bond occurs when there is evidence of a net attractive interaction between an electrophilic region associated with a halogen atom in a molecular entity and nucleophilic region in another, or the same, molecular entity [46]"

The halogen bonding phenomena has not been much studied with respect to photoisomerization of the azo-polymer complexes but in recent years it has gain much attention with promising results [47]. The intermolecular interactions developed by the electrophilic halogens were projected as the "halogen bond". The halogen bonding phenomenon has been defined and termed in multiple different ways but cannot be established its exact occurrence date. Depending on the properties of the starting molecules and according to different aspects of the intermolecular interactions, as the main factor of intermolecular interactions is the increased nucleus-electron attraction. The interactions based on molecular properties can be termed as "points in holes" and "locks in keys" etc. and highlighting the different aspects as saturation of bonding potential and directional character of intermolecular interactions. On the bases of the intermolecular interactions in F—Cl---F—H complex, it is termed as the "anti-hydrogen bond" to highlight the difference regarding hydrogen bond [48].

Figure 3.3: *Schematic representation of Halogen Bond, (R = C, N, Halogen), (X = F, Cl, Br, I), (Y = N, O, S, Se, F^-, Cl^-, Br^-, I^-) [48]*

The halogen bonding is like hydrogen bonding, a non-covalent interaction where electron density acceptor is a Halogen atom [17]. The dissimilarities of XB with HB surface the importance and capacity of XB rather than the similarities. The prominent dissimilarities can explain the XB with the differences of the directionality, hydrophobicity, tunability and donor atom size to HB. Considering directionality, where the positive electrostatic potential, the σ-hole, present on the outermost surface of the halogen atom. This positive electrostatic potential is resultant of the interaction between electronegative halogen atom and the strong electron withdrawing part of the molecule, when the electrons of the halogen atom are withdrawn towards the molecule a small positive spot appears on halogen atom opposite to the location where it bonds with the molecule, this positive spot is called σ-hole [2]. The σ-hole can be explained too: as shared electron density of X-atom defines the XB interaction, because of that the distribution of the

density exists along the equatorial area of the bond, which leaves the polar area of the bond unfilled and void, this form of distribution is called σ-hole [17].

The positive region of the HB donors is more spread over the surface of hydrogen atom while the σ-hole is barely retrained to the R—X covalent bond axis elongation. It illustrates that comparative to HB, with classic R—X---Y bond, the XB tends to be more directional, where Y is any nucleophilic site [47]. The strengthening of σ-hole occurs with the polarizability of the halogen atom and with the electron extracting capacity of the moiety to which the halogen is attached. The bond strength is established in the order that the strength increases for more polarizable halogens such that I>Br>Cl >F, where the F atom only acts as a halogen bond donor when connected to strong electron-extracting groups (e.g. $F_{2n+1}C_n$—I or F_5C_6—I) due to its low polarizability but the chemical environment of the of the atoms involved affects the bonding strength as well. The example of carbon hybridization next to X-atom can be taken to understand it as: C≡C—X > C=C—X > R—C—X. In the case of FCN, the F-atom is expected to have on its surface a completely positive electrostatic potential which can assist the formation of the halogen bonded complexes like H_3N---FCN and FCN---FCN. It leads to that the strongest bond in case of F—X molecules will be with F—I and with F—Cl the weakest one. This differentiates it from the HB as it can be tuned through single atom mutation [17] [47] [48].

In 20th century ground breaking experimental observations have been reported for which the XB role has been acknowledged well today. The first case of intermolecular donor acceptor interactions later rationalized this phenomenon in 1948. In 1952, subclass of the electron acceptor-donor complex family was classified, two years after similar complexes were reported including carbonyl derivatives, ethers and thioethers. UV-vis spectroscopy specified that in all these complexes, even the weaker ones, a charge transfer to halogen occurs such as including di-halogens and aromatics or perfluorocarbons and amines [48].

In this study the halogen dyes used are based on I atoms and by the presence of highly electronegative F-atoms in the perfluoro-benzene ring I-atoms behave more electron poor and this effect is facilitated by the delocalization of electrons in aromatic ring.

4. EXPERIMETNAL WORK

4.1 Materials

In this experimental work we studied both hydrogen and halogen bonded complexes by using different molecular masses of one kind of polymer to understand, study and compare the effect and behavior of different dyes with different polymeric weights of same kind. The structure of the dyes can be seen in the Figure 4.1.

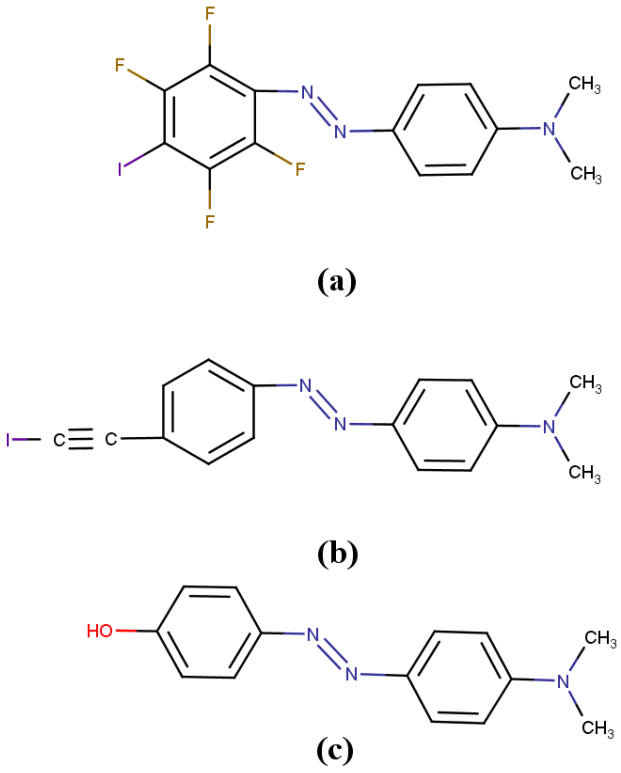

Figure 4.1: *Azo-Chromophores Structures (a) Azo-I (b) Azo-T (c) 4-Hydoxy*

The azobenzene (a) in the Figure 4.1, donated as **Azo-I**, is a per-fluorinated azo dye with iodine as the halogen bond donor and the azobenzene (b) in the Figure 4.1, **Azo-T**, has an iodo-ethynyl substitution group providing the *σ-hole* necessary for halogen bonding. Both halogen-bond-donating dyes are similar in interaction strength but with different charge distribution and molecular shapes [2]. The azobenzene (c) in the Figure 4.1, called here, **4-hydoxy**, forms hydrogen bond when introduced to a polymer matrix.

The polymer used in this study is Poly(4-vinylpyridine) (P4VP, an amorphous polymer, which is very common in the study of supramolecular photoactive polymer complexes

formation and it acts for both hydrogen and halogen bonding as an acceptor. The structure of the P4VP is shown in the Figure 4.2

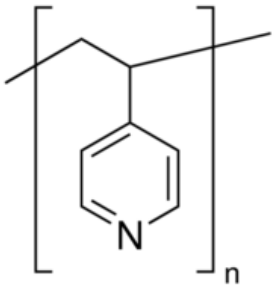

Figure 4.2: *Poly(4-vinypyridine), Amorphous polymer.*

The experiments were designed for different weights of P4VP, ranging as 1kD, 1.8kD, 2.3kD, 3.2kD, 4.3kD and 7kD against three chromophores two based on halogen bonding and one based on hydrogen bonding to compare the effect of the bonding and the weight of the polymer on the SRG formation efficiency.

Mixture of two different solvents was used in this study to dissolve the complexes and spin coat the thin film samples, Dimethylformamide (DMF) and Chloroform ($CHCl_3$) used in specific ratios to make a solvent mixture. DMF highly polar and chloroform is less polar relative to DMF. The mixture of two solvents used as some of the complexes were not soluble in the $CHCl_3$ alone, so a mixture of $CHCl_3$ and DMF was necessary with a ratio at which the complexes were soluble. After trials, the required ratio was determined and proved to be feasible for the experiments.

4.2 Sample Preparation

The experimental work can be categorized into two sections, in the first section the polymer weight is kept constant and the effect of increasing mol% of the dye is studied, in the second section the dye is kept constant and the effect of the increasing polymer weight on the phenomena is studied. All the samples were prepared with a molar concentration of 1 mol-%, 3.3 mol-%, 5 mol-% and 10 mol-%. For instance, 1 mol-% and 10 mol-% refer to case where 100^{th} and every 10^{th} polymer repeat unit (P4VP) is occupied by an azobenzene molecules, respectively.

All the samples prepared in the solvent mixture of (Chloroform: DMF), the mother solutions for both polymer and dyes were prepared at specific concentration determined in weight percentage. The solutions were mixed at the desired amounts to prepare the required complexes. The microscope glass slides cut into 38mm sized substrates in length were used.

4.2.1 Solution preparation:

The solvent is prepared by mixing $CHCl_3$ and DMF in a 60:40 to dissolve the azo-polymer complexes. The solution of the dye and polymer were prepared in 8 wt-% and mixed at desired complex ratios. The molecular weight of P4VP is 105.14, the weight of **Azo-I** is 423.15, molecular weight of **Azo-T** is 375.21 and molecular weight of **4-hydroxy** is 241.29 g/mole. The basic steps used to calculate the formulation are as following (an example table which was used for each of the studied complex solutions).

For Polymer/Dye Wt%:

Wt% required=___, Molecular weight=___,

Weight of Dye/Polymer taken (mg)=_____

Amount of Solvent required = $\frac{Weight\ of\ Polymer}{Weight\ \%}$ =_____(mg)

(Polymer + Dye) Solution with _X_ Mol% of Dye (X = _____):

Dye solution taken = _____ mg dye wt% = _____

So ➔ Mass of dye = amount of dye solution taken × Wt% = _____ mg of dye

To add Proper amount of polymer solution,

Dye mass fraction = $\frac{X \times molecular\ wt\ of\ Dye}{(X \times molecular\ wt\ of\ dye) + molecular\ wt\ of\ polymer}$ = _____.

Overall mass of Polymer + Die = $\frac{mass\ of\ dye}{dye\ mass\ fraction}$ =_____mg

Mass of polymer = (Overall mass of polymer + die) – mass of dye =_____mg

Amount of Polymer solution to be taken = $\frac{mass\ of\ polymer}{wt\%\ of\ polymer\ solution}$ =_____ mg

4.2.2 Cutting and Cleaning the Substrate

The 76mm long, 26mm wide and 1mm thick microscope glass slides used in this study. The slides are cut into half which makes one substrate of 38mm in length. After cutting the substrates are washed and cleaned with sonication and then dried in the oven with following steps described below,

The glass substrate used can be seen in the Figure 4.3

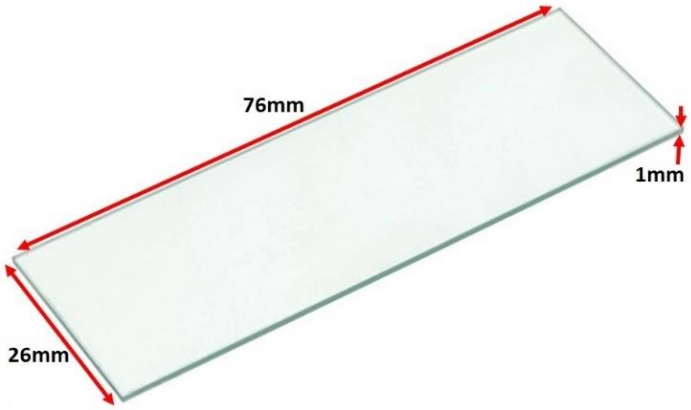

Figure 4.3: *Microscope glass Slide of length 76mm, width 26mm and thickness 1mm*

- Measure and Cut the glass substrates (76mm) from center, almost 38 mm each in length.
- Fill the container with acetone above the glass substrate height and place it in the ultrasonic bath with a frequency of 37 kHz with 50% power at 45 C for 15 min. After 15 min pour out acetone.
- Fill the container with Isopropyl Alcohol (propanol) above the substrate height and place the container in bath with same frequency, power, temperature and time. After 15 min pour out propanol.
- Fill the container with Milli-Q (highly pure water) above the substrate height and place it in the bath again at same frequency, power, temperature for 15min. after 15 min pour out the Milli-Q and take out the substrate holder.
- Dry the substrates with nitrogen flow.
- Place the substrates in the oven at 70 C for 90 minutes. After drying, the samples are ready to use and store.

4.2.3 Spin Coating and Drying

In spin coating, the speed and rotations per minute or round per minute (RPM) have been different for couple of samples to increase the thickness of coating. In general, almost all the samples were prepared at 800 and 500 acceleration and RPM with the below parameters:

Nitrogen Pressure = 4.2 bar Solution Taken = 200 µL

Step # 1

RPM = 400 to 800 Acceleration = 400 to 800 Time = 20 to 30 sec.

Step # 2

RPM = 500, Acceleration = 500, Time = 2 min.

Drying:

All the spin coated thin film samples were dried at 70 ˚C for 60min in the oven.

4.2.4 Film Thickness and Absorption Spectrum

The UV-Visible absorption spectrum of the samples was measured by the spectrophotometer. The samples were placed at normal incidence to the incoming light beam and the reference spectrum was measure by placing the clean microscopic glass slide (Figure 4.3).

The film thickness of one sample out of each category of compositions of polymer and chromophores was measured by profilometer in the TUT clean room laboratory facilities, which were used as the reference sample to measure the thickness of the remaining samples of same category and class by the absorption spectrum measurements. The higher the absorption, the thicker is the film. One such example is quoted in the following calculations

Reference Sample # (E-1) (4-Hydroxy + P4VP-1000) (10 Mol% of Dye)

Absorption of New Sample = 1.295, Wavelength of Max Absorption = 415,010

Absorption of Reference Sample = 1.240,

Thickness of Reference Sample = 695.02 nm,

$$A = \frac{Absorption\ of\ Reference\ sample\ (A1)}{Absorption\ of\ New\ sample\ (A2)} = \frac{1.240}{1.295} = 0{,}957 \rightarrow \mathbf{A}$$

$$\text{Thickness of New Sample} = \frac{\boldsymbol{Thickness\ of\ reference\ Sample}}{\boldsymbol{A}} = \frac{695.02}{0{,}957} = \mathbf{726{,}91\ nm}$$

The thickness of all the samples measured with the application of the beer law as explained above, which states as

$$A = \varepsilon.\ c.\ b, \rightarrow \varepsilon = \frac{A}{cb} \rightarrow b = \frac{A}{c\varepsilon}$$

Where, Ɛ = molar absorptivity, c = concentration, b = thickness, A = absorbance.

The concentration of the chromophores used are mentioned in mol% and weight % in the Table 4.1.

Table 4.1: *Dye Concentrations for 4-Hydroxy, Azo-I, Azo-T*

Dye Concentration for 4-Hydroxy	
Degree of Complexation, X (mol %)	**weight %**
10 Mol %	**18.67**
05 Mol %	**10.29**
3.3 Mol %	**7.04**
02 Mol %	**4.39**
01 Mol %	**2.24**
Dye Concentration for Azo-I	
Degree of Complexation, X (mol %)	**weight %**
10 Mol %	**28.70**
05 Mol %	**16.75**
3.3 Mol %	**11.72**
02 Mol %	**7.45**
01 Mol %	**3.87**
Dye Concentration for Azo-T	
Degree of Complexation, X (mol %)	**weight %**
10 Mol %	**26.30**
05 Mol %	**15.14**
3.3 Mol %	**10.54**
02 Mol %	**6.66**
01 Mol %	**3.45**

The thickness of the reference samples measured by profilometer with stylus force of 1mg and stylus type of 50 nm radius for the duration of 60 seconds with profile Hills and valleys for the length of 2000 µm to 3000 µm. the reference sample thicknesses later used to measure the thickness of the other sample with values of absorption spectrum by using Beer's law and dye concentration (c) is taken in wt% to calculate the molar absorptivity.

Table 4.2: *Film Thickness calculation of the samples with reference to absorption spectrum samples*

Sample No.	Wavelength (nm)	Abs = A	c.ε	Thickness (nm) = b
10X-01kD	413.01	1.240	0.00178	696.11
10X-1.8kD	415.01	1.295	0.00178	726.91
10X-2.3kD	414.01	1.330	0.00178	746.58
10X-3.2kD	414.01	1.314	0.00178	737.52
10X-4.3kD	415.01	1.366	0.00178	766.81
10X-07kD	413.01	1.537	0.00178	862.44
05X-01kD	414.01	0.709	0.00098	722.08
05X-1.8kD	415.01	0.661	0.00098	673.27
05X-2.3kD	414.01	0.706	0.00098	718.52
05X-3.2kD	415.01	0.717	0.00098	729.75
05X-4.3kD	415.01	0.705	0.00098	718.37
05X-07kD	414.01	0.794	0.00098	808.15
03X-01kD	414.01	0.462	0.00067	687.00
03X-1.8kD	415.01	0.481	0.00067	716.25
03X-2.3kD	414.01	0.498	0.00067	741.08
03X-3.2kD	415.01	0.496	0.00067	737.89
03X-4.3kD	415.01	0.478	0.00067	711.31
03X-07kD	414.01	0.547	0.00067	814.19
02X-01kD	416.00	0.277	0.00042	661.16
02X-1.8kD	416.00	0.245	0.00042	585.71
02X-2.3kD	415.00	0.250	0.00042	597.65
02X-3.2kD	416.00	0.245	0.00042	584.05
02X-4.3kD	416.00	0.257	0.00042	614.41
02X-07kD	415.00	0.357	0.00042	851.51
01X-01kD	415.01	0.134	0.00021	626.09
01X-1.8kD	415.01	0.133	0.00021	621.00
01X-2.3kD	414.01	0.135	0.00021	633.12
01X-3.2kD	416.01	0.159	0.00021	741.86
01X-4.3kD	417.01	0.132	0.00021	619.66
01X-07kD	415.01	0.170	0.00021	795.06
02X-Azoi-01kD	464.99	0.239	0.00021	1148.19
02X-Azoi-1.8kD	469.98	0.253	0.00021	1215.66
02X-Azoi-3.2kD	469.98	0.241	0.00021	1154.53
02X-AzoT-01kD	450.99	0.414	0.00036	1147.10
02X-AzoT-1.8kD	454.01	0.350	0.00036	968.36
02X-AzoT-3.2kD	449.99	0.421	0.00036	1164.74

Where: samples from 10X-01kD to 01X-07kD are complexes of 4-hydroxy and P4VP from 1kD to 7kD at different complexation (X) ratios from 10 mol% to 01 mol%. The last six samples are complexes of **Azo-I** and **Azo-T** with P4VP at 02 mol%, as indicated in the sample names (e.g. 10X-01kD: → 10 = X value in mol%, 1kD = polymer weight).

4.3 Surface Relief Gratings (SRGs) Formation:

The formation of the SRGs is the resultant of photoisomerization of the chromophores of nanometer size which can perform broad scale mass migration of the polymer chains over a significant distance of several microns [3]. The experimental setup used for the inscription of SRGs is illustrated in the Figure 4.4. to create interference pattern half of the beam is required to be projected directly on the sample (S) while the other half is being reflected by the mirror against which the sample is placed at right angle. The surface relief gratings process is very complex, and the nature of the material system and the experimental arrangement setup highly affects the efficiency of the process [3].

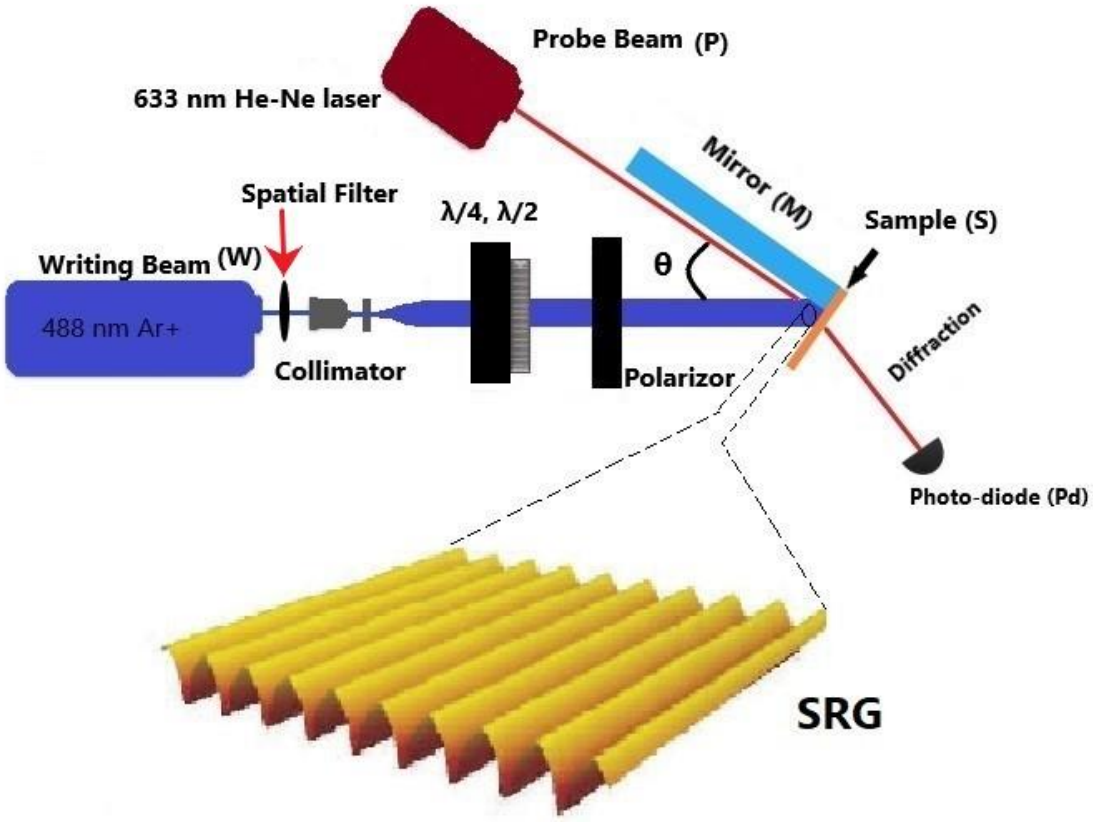

Figure 4.4: *Laser Setup for the inscription of SRGs [3] Figure adopted from [49]*

The spatial filter controls the quality of the beam by cleaning and expands the light as it passes through it. The polarization of the inscription beam is determined by the wave plate and polarizer, as quarter wave plate provides the circular polarization as used in the study of this work. The intensity or power of the beam is determined by the half wave plate or the power regulator. The area of the inscription on sample is determined by the iris radius to give specific path to the beam for gratings and controls the light required for grating. The higher the annotation of light, lower the intensity of the light and reduced size of irradiated area means higher value of irradiation.

The inscription beam or the writing beam was 488 nm Ar^+ laser, in blue/purple color and the probe beam was 633 nm Ge-Ne laser, in red color. The Writing beam creates the surface relief gratings while the probe beam is used to measure the diffraction as the probe beam reaches the photodiode. The quality of the SRGs formation determines the value of the diffraction efficiency. The probe beam is used to measure the diffraction efficiency as the wavelength of the beam is outside the absorption range of the azobenzenes selected for this study and thus the beam diffracts from the sample surface due to the SRGs formation [2]. The first order and the second order diffraction can be measured in real time by the power meter if the grating spacing is large enough, larger the grating spacing higher the value of the diffraction [3]. The setup path of the Ar^+ laser beam can be seen in the below as set up in lab

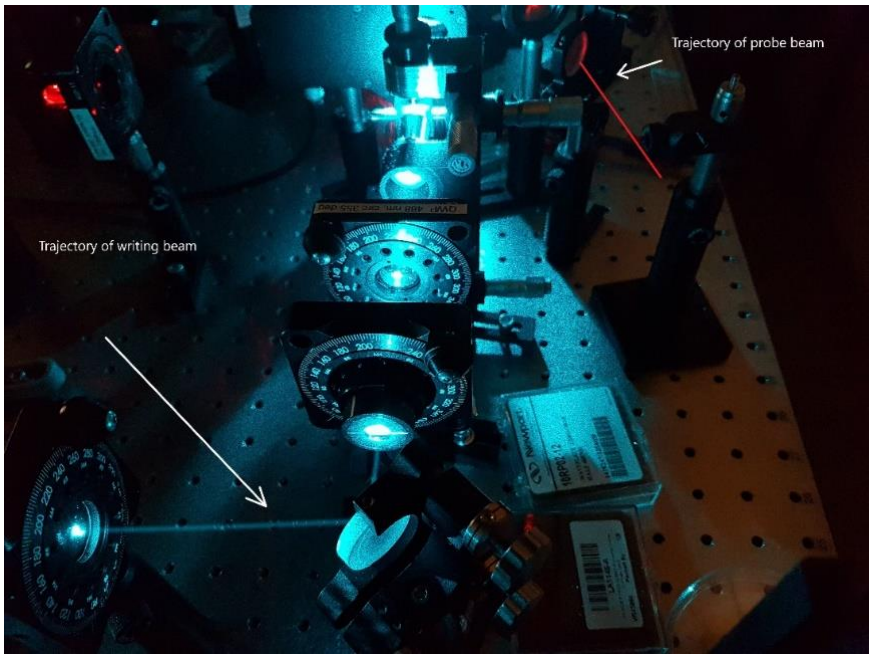

Figure 4.5: *488 nm Ar^+ laser setup in lab*

The fringe spacing ʌ for the interference pattern created can be determined by the angle between the samples normal (θ) and the beam axis of propagation, which is stated as

$$\Lambda = \frac{\lambda}{(2Sin\ \theta)}$$

where the λ is the wavelength of the inscription beam/writing beam or the irradiation beam.

A good grating requires precise setup of the laser equipment to assure the accurate values for the inscription and probe beam with sufficient power and intensity. The power, intensity, area of study on sample, iris radius and angle are very crucial parameters in the laser setup. In this study an angle of 15° was used as at this angle SRG formation is

considered very efficient. The power and intensity calculations were carried out with the following method

Iris Diameter = 6,31 mm = $\frac{6.31}{10}$ = 0,631 cm,

Iris Radius = $\frac{Iris\ Diameter}{2}$ = $\frac{0.631}{2}$ = 0.3155cm ➔ **r**

Intensity, I = 300 mw/cm^2, I = $\frac{P}{A}$ ➔ P = I × A ➔ A = πr^2

P = 93,8 mw ≈ 94 mw Inscription Time = 65 min.

The iris diameter calculated with the Vernier caliper and 300 mw/cm^2 is considered an efficient intensity to form the SRGs and the power of the irradiation beam is calculated to attain the required intensity of the beam. The SRG formation time given was 65 minutes with the power of ≈94 mw.

4.3.1 Measuring Real Time Diffraction

The real time diffraction is measured with the power meter, first the power of the incident probe is measured and then the power of the diffracted probe is measured and by dividing the diffracted probe by incident probe and multiplying it by 100 gives the real time diffraction efficiency, as shown in the example below.

Incident Ray ➔ R_i = 4.1 mw, Diffracted Ray ➔ R_d = 0.8 mw

Diffraction Efficiency ➔ η = $\frac{Diffracted\ Ray}{Incident\ Ray}$ =19.5%

The polarization of the inscription beam highly affects the efficiency of SRG formation. Circular polarization is considered to provide most efficient rate of grating inscription for the materials studied in this work. With circular polarization the periodic polarization is aroused by the interference pattern and in intensity only weak modulation. This statement does not fulfill for all the dyes as for some azo-polymer complexes the largest surface modulation is aroused by the p-polarized inscription beam [3]. In the Figure 4.6, the diffraction efficiencies of azo-polymer complexes of 4hydroxy-P4VP can be seen with different weights of P4VP.

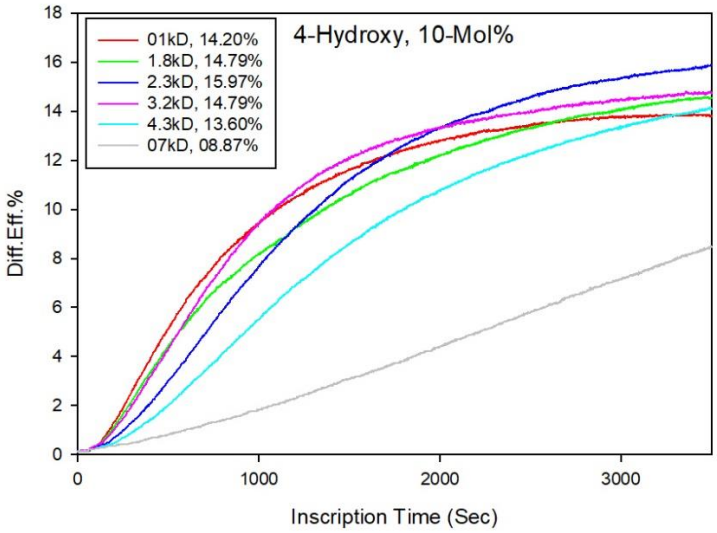

Figure 4.6: *Real time diffraction efficiencies of 4-hydroxy-P4VP (at X = 10 mol%)*

The grating formation and measurement of real time diffraction efficiencies leads towards the study of modulation depth of the gratings with atomic force microscopy (AFM) images as shown in the Figure 2.10. The dye concentration and the sample thickness are important factor to determine the gratings height as stated earlier too.

5. RESULTS AND DISCUSSION

5.1 Sample Quality

To study the properties and behavior of azo-polymer complexes under light illumination, thin film samples are considered to be most suitable to conduct the study. The thin coating/film preparation is carried out with spin coating. The speed and acceleration of the coating process can determine the thickness of the film. The transparent glass substrates are used to form thin coatings.

Poly(4-vinylpridine) polymer (P4VP) was used with different grades to form complexes with three different chromophores **4-hydroxy, Azo-I, Azo-T** as already mentioned in the previous section. A sample solution with required amounts of the polymer and azobenzene was prepared to spin coat the substrates. All the samples coated with an amount of 200 µL and allowed the samples to dry at room temperature and covered the samples during drying process so that the dust particles do not accumulate on the surface and affect the quality of the samples.

The role of solvent choice is very prominent in the azo-polymer complexes as it affects the quality of samples. The sample preparation scheme in the beginning was supposed to be designed with chloroform as solvent but all the selected polymers and dyes did not dissolve in 100% chloroform solvent. The phase separation observed after mixing the materials in the chloroform and it did not provide enough time to make a good quality sample, as the samples made of it showed crystallization and large particle accumulation after some time. To overcome this problem a mixture of chloroform and DMF used, first an 80:20 (chloroform: DMF) was used which did not work out and after some trials a ratio of 60:40 (chloroform: DMF) resulted to be suitable for the designed experiments and all the materials proved fully soluble in the solvent mixture.

In Figure 5.1, two different solvents are shown with same type of dye, it can be clearly seen that in solvent (b) the dye is fully soluble which contains a mixture of two solvents Chloroform and DMF with a ratio of 60:40 respectively. The dye in solvent (a) can be seen insoluble which is chloroform only, and large insoluble particles of the dye can be seen on the walls of the bottle and in the solution as well.

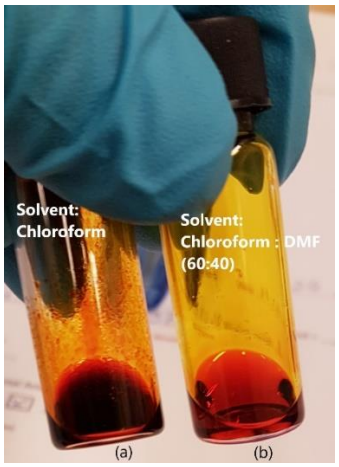

Figure 5.1: *Solubility of one dye in (a) Chloroform (100%) and (b) Chloroform: DMF (60:40)*

The samples prepared with the spin coating process can be seen in the Figure 5.2.

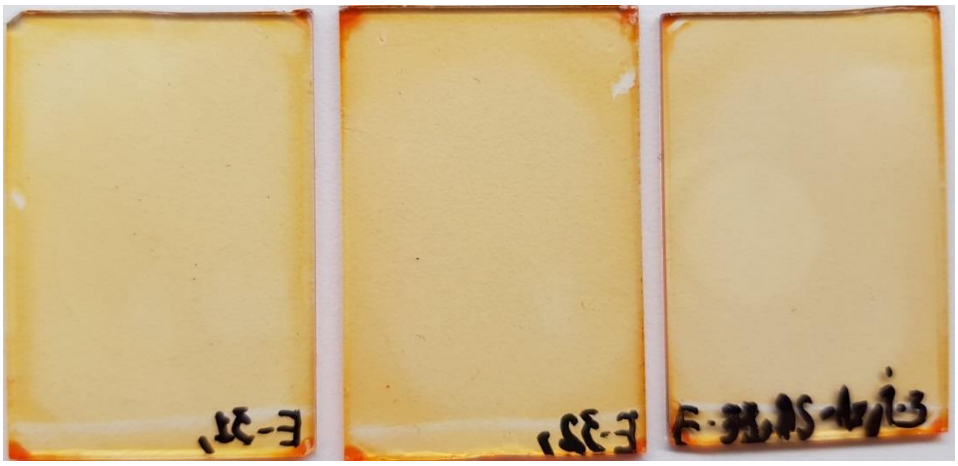

Figure 5.2: *Spin Coated samples of Azo-I*

The solution coated on the glass substrate provided good quality film and good thickness.

5.2 UV-Vis Spectrum

The UV-Vis spectra of the azo-polymer films are plotted in the following figures. Which includes, **4-hydroxy** (Figure 5.3), **Azo-I** (Figure 5.4. a) **Azo-T** (Figure 5.4. b) and comparison of the absorption spectrum of hydrogen bonded and halogen bonded complexes is given in Figure 5.5.

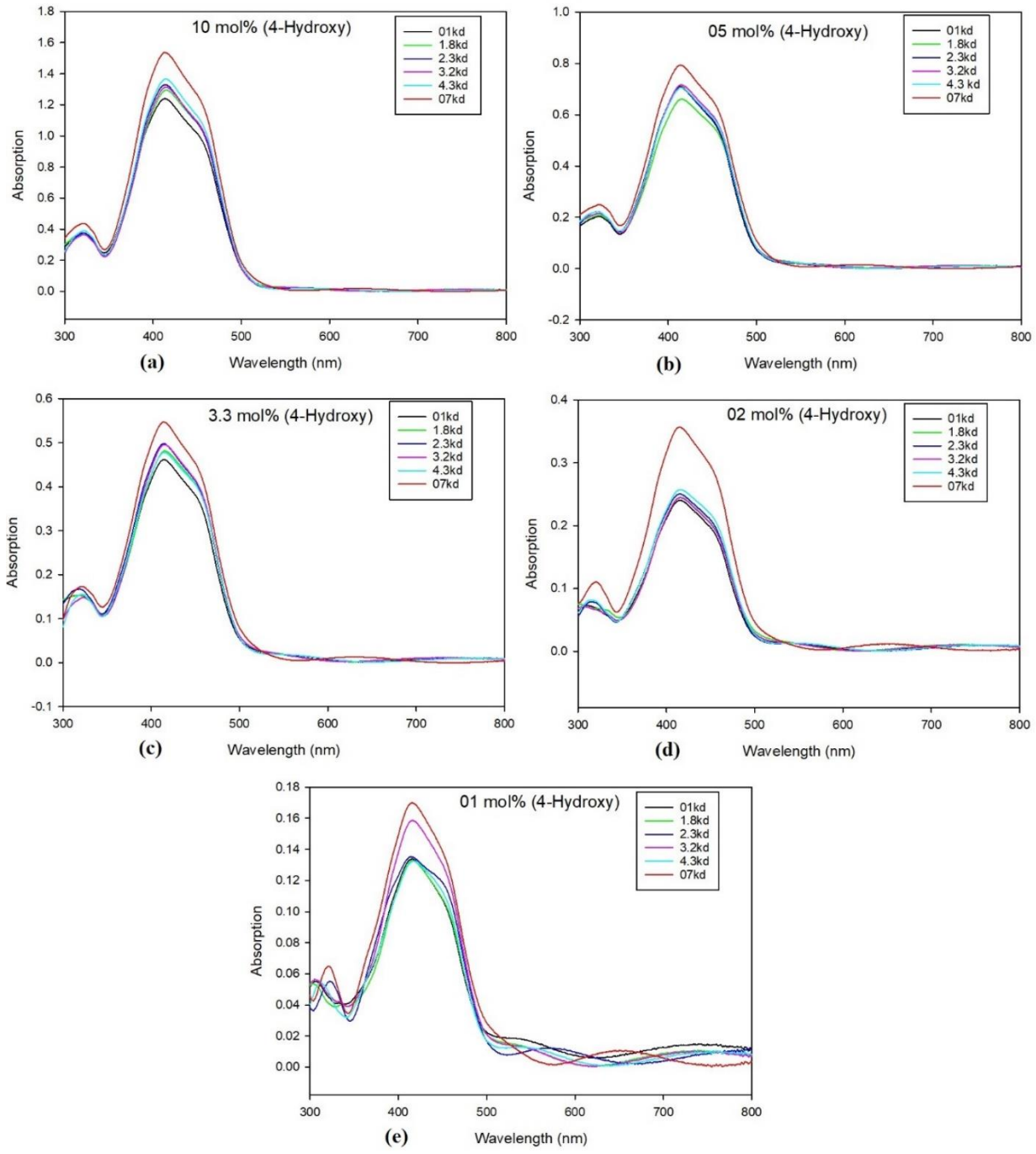

Figure 5.3: *Absorption spectrum of 4-hydroxy (a) 10 mol% (b) 05 mol% (c) 3.3 mol% (d) 02 mol% (e) 01mol%, all in Polymer P4VP*

The maximum wavelength of absorption (λ_{max}) for 4-hydroxy-polymer complexes (Figure 5.3) does not show much spectrum shift for all the dye concentrations. The λ_{max} of absorption for **4-hydroxy** lies between 413 nm to 416 nm (Table 5.1) upon increasing the concentration. Moving from lower to higher (01 mol% to 10 mol%) chromophore concentration of **4-hydroxy**. For conventional guest-host systems, it is expected that the aggregation take place with increase in dye concentration and aggregation gives rise to a distinct peak at lower wavelength [3].

For hydrogen bonded (Figure 5.3) azo-polymer complexes, as a common trend, the absorption increases with an increase in the dye concentration and molecular weight. For absorption (Table 5.1) of 4-hydroxy-polymer complexes, we can conclude that the dye concentration and the polymer weight are directly proportional to each other.

Table 5.1: *Maximum wavelengths of absorption for polymer complexes containing 4-hydroxy, Azo-I and Azo-T*

Sample No.	Wavelength (nm)	Abs = A
10X-01kD	413.01	1.240
10X-1.8kD	415.01	1.295
10X-2.3kD	414.01	1.330
10X-3.2kD	414.01	1.314
10X-4.3kD	415.01	1.366
10X-07kD	413.01	1.537
05X-01kD	414.01	0.709
05X-1.8kD	415.01	0.661
05X-2.3kD	414.01	0.706
05X-3.2kD	415.01	0.717
05X-4.3kD	415.01	0.705
05X-07kD	414.01	0.794
03X-01kD	414.01	0.462
03X-1.8kD	415.01	0.481
03X-2.3kD	414.01	0.498
03X-3.2kD	415.01	0.496
03X-4.3kD	415.01	0.478
03X-07kD	414.01	0.547
02X-01kD	416.00	0.277
02X-1.8kD	416.00	0.245
02X-2.3kD	415.00	0.250
02X-3.2kD	416.00	0.245
02X-4.3kD	416.00	0.257
02X-07kD	415.00	0.357
01X-01kD	415.01	0.134
01X-1.8kD	415.01	0.133
01X-2.3kD	414.01	0.135
01X-3.2kD	416.01	0.159
01X-4.3kD	417.01	0.132
01X-07kD	415.01	0.170
02X-Azoi-01kD	464.99	0.239
02X-Azoi-1.8kD	469.98	0.253
02X-Azoi-3.2kD	469.98	0.241
02X-AzoT-01kD	450.99	0.414
02X-AzoT-1.8kD	454.01	0.350
02X-AzoT-3.2kD	449.99	0.421

The maximum wavelengths of absorption are given in the Table 5.1, for all the dye concentrations.

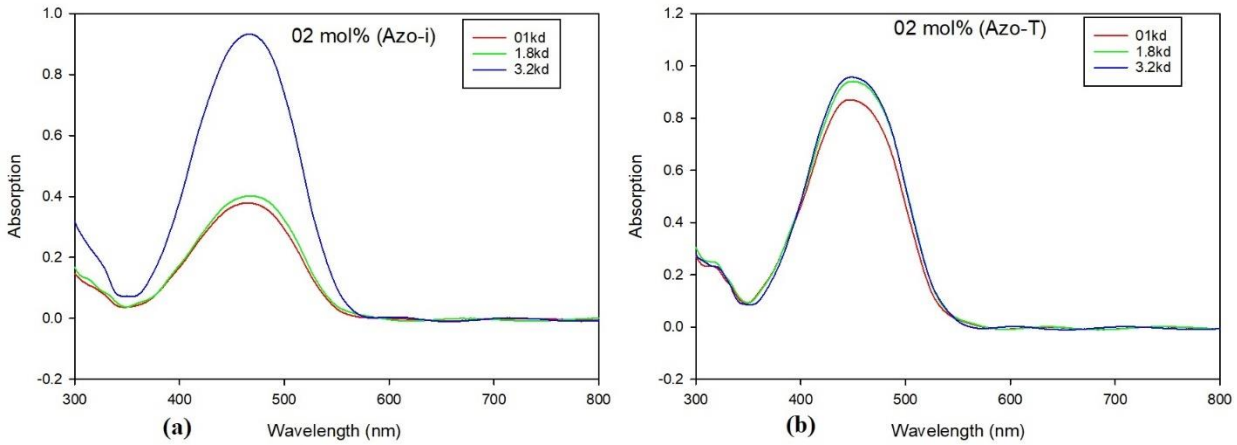

Figure 5.4: *UV-Vis Spectrum of (a) Azo-I (b) Azo-T at 02 mol% dye concentrations in P4VP*

For the λ_{max} of absorption for **Azo-I** (Figure 5.4. a) show minimal spectrum lies between 465 nm to 470 nm (Table 5.1) and the curve peaks are very smooth and isolated, which indicates no chromophore aggregation. For **Azo-T** the λ_{max} lies 450 nm to 454 nm, also the curve peaks are very smooth and indicate no distinct peaks and no chromophore aggregation.

For both halogen bonded (Figure 5.4) azo-polymer complexes, the absorption pattern does not follow the trend that the higher the polymer weight, higher is the absorption and same follows for low the molecular weights. It can be seen in Table 5.1 and Figure 5.4Figure 5.3 for the polymer's molecular weights. It is evident that each polymer molecular weight behaves differently for the halogen bonded-complexes without a trend. The smooth curves with no prominent spectrum shifting of λ_{max} of absorption indicates that no chromophore aggregation occur and chromophores are well dispersed in the polymer matrix [2] [50]. The λ_{max} of absorption is not only depended on the dye concentration (X-value) but it is also affected by the sample thickness and the solvent polarity [10]. When the chromophores are incorporated into polymers, the polymers can be considered as solvents too [10].

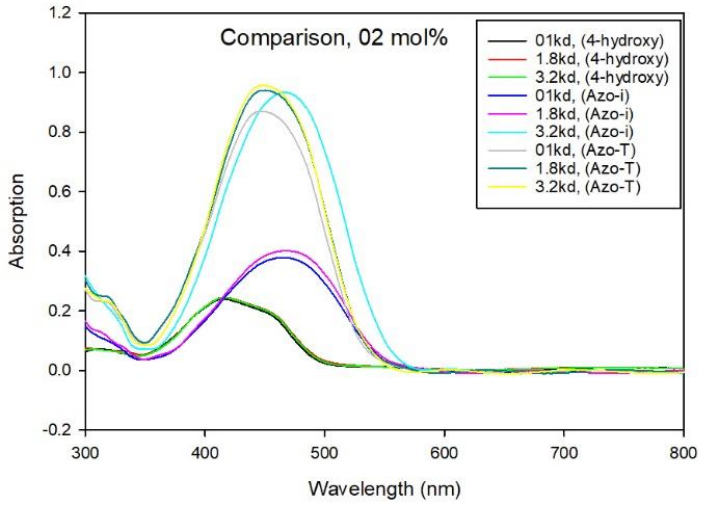

Figure 5.5: *UV-Vis spectra Comparison of* ***4-hydroxy****, Azo-I and Azo-T*

The comparison of the three azobenzene chromophore (X = 02mol%) as shown in the Figure 5.6. Which indicates that the **Azo-I** and **Azo-T** has the higher absorption spectrum comparative to the **4-hydroxy** absorption spectrum with same dye concentration, but all have different range of λ_{max} of absorption. It also indicates that for both hydrogen-bonded and halogen bonded complexes the chromophore aggregation is very minimal, and chromophores are well dispersed in the polymer matrix. The isolated peaks indicate better *trans-cis* isomerization as in *trans*-azobenzenes the strong aggregation tends to restrain their conformational changes and hinders *trans-cis* isomerization which [3]. The P4VP is polar and within polymer chains, the polar functional group allows the monomer concentration to be increased without aggregation, although between the polymer and dyes, relatively weak intermolecular interactions are expected [3].

The dye concentrations used in this study are assumed not to cause the chromophore aggregation as observed in Figure 5.3. As observed in earlier work of Priimägi *et al*. [3], at 30 wt% of the DR1 chromophore aggregation was reported. In our study the maximum dye concentration is 10 mol% and the corresponding weight % are given in Table 4.1 for each dye.

5.3 SRG Diffraction Efficiencies

The first order SRG formation diffraction efficiencies are shown in the figures below for respect to the polymer molecular weight (Figure 5.6) and the chromophore concentration (Figure 5.7) in the polymer matrix. For all the complexes the grating inscription intensity of 300 mw/cm^2 used. The final diffraction efficiencies after blocking the inscription beam are enlisted in the Table 5.2.

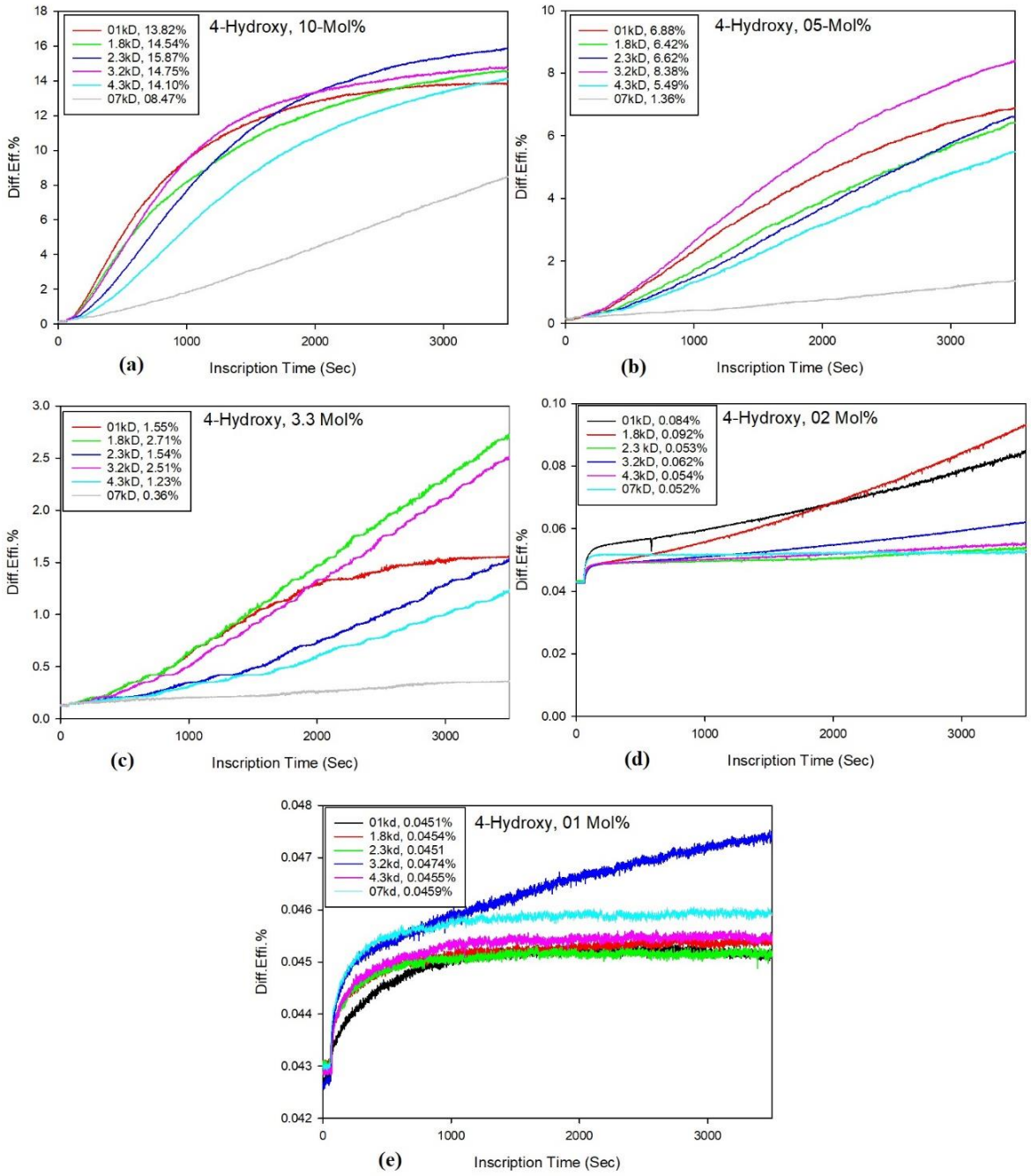

Figure 5.6: *Evolution of diffraction efficiencies for different concentration values (X) of 4-Hydroxy (a) 10 mol% (b) 05 mol% (c) 3.3 mol% (d) 2 mol% (e) 1 mol%*

The hydrogen bonded complexes of **4-hydroxy** and P4VP are represented in the Figure 5.6. Priimägi *et al*. [18] has already published the similar work which is also reference to this study. We extended the study to different molecular weights (1kD to 7kD) with different dye concentrations (1 mol% to 10 mol%). Here; 1 mol% indicates that 1 azobenzene molecule per 100 polymer repeat unites and for 10 mol%, 1 azobenzene molecule per 10 polymer repeat units [18]. The previous work study proved the 4-hydroxy-P4VP complexes an efficient azo-polymer complex for SRG inscription and our work study showed similar outcomes as shown in Figure 5.6 [18].

Table 5.2: *Diffractions Efficiencies for all the dye concentrations and polymer weights*

Sample No.	Thickness (nm)	Diff. Effi.%
10X-01kD	696.11	13.826
10X-1.8kD	726.91	14.547
10X-2.3kD	746.58	15.875
10X-3.2kD	737.52	14.758
10X-4.3kD	766.81	14.103
10X-07kD	862.44	8.477
05X-01kD	722.08	6.880
05X-1.8kD	673.27	6.429
05X-2.3kD	718.52	6.623
05X-3.2kD	729.75	8.382
05X-4.3kD	718.37	5.493
05X-07kD	808.15	1.360
03X-01kD	687.00	1.553
03X-1.8kD	716.25	2.717
03X-2.3kD	741.08	1.547
03X-3.2kD	737.89	2.511
03X-4.3kD	711.31	1.233
03X-07kD	814.19	0.362
02X-01kD	661.16	0.085
02X-1.8kD	585.71	0.093
02X-2.3kD	597.65	0.053
02X-3.2kD	584.05	0.062
02X-4.3kD	614.41	0.055
02X-07kD	851.51	0.052
01X-01kD	626.09	0.045
01X-1.8kD	621.00	0.045
01X-2.3kD	633.12	0.045
01X-3.2kD	741.86	0.047
01X-4.3kD	619.66	0.046
01X-07kD	795.06	0.046
02X-Azoi-01kD	1148.19	0.276
02X-Azoi-1.8kD	1215.66	0.352
02X-Azoi-3.2kD	1154.53	0.351
02X-AzoT-01kD	1147.10	1.210
02X-AzoT-1.8kD	968.36	1.291
02X-AzoT-3.2kD	1164.74	0.821

The 4-hydroxy-P4VP complexes show systematic increase in the diffraction efficiencies with an increase in the chromophore concentration as shown in Table 5.2. The diffraction efficiency values obtained at 1 mol% as well with small values (Table 5.2) and

quick saturation. As indicated in previous works [18] that 1 mol% (Figure 5.6 e) is the smallest studied concentration at which the SRG formation occurs and the thickness of the film only affects the light induced mass transport efficiency. This result endorses the study work conducted by Priimägi *et al.* [18] stating that for mass transport to be induced not every polymer chain has to carry the chromophore molecule.

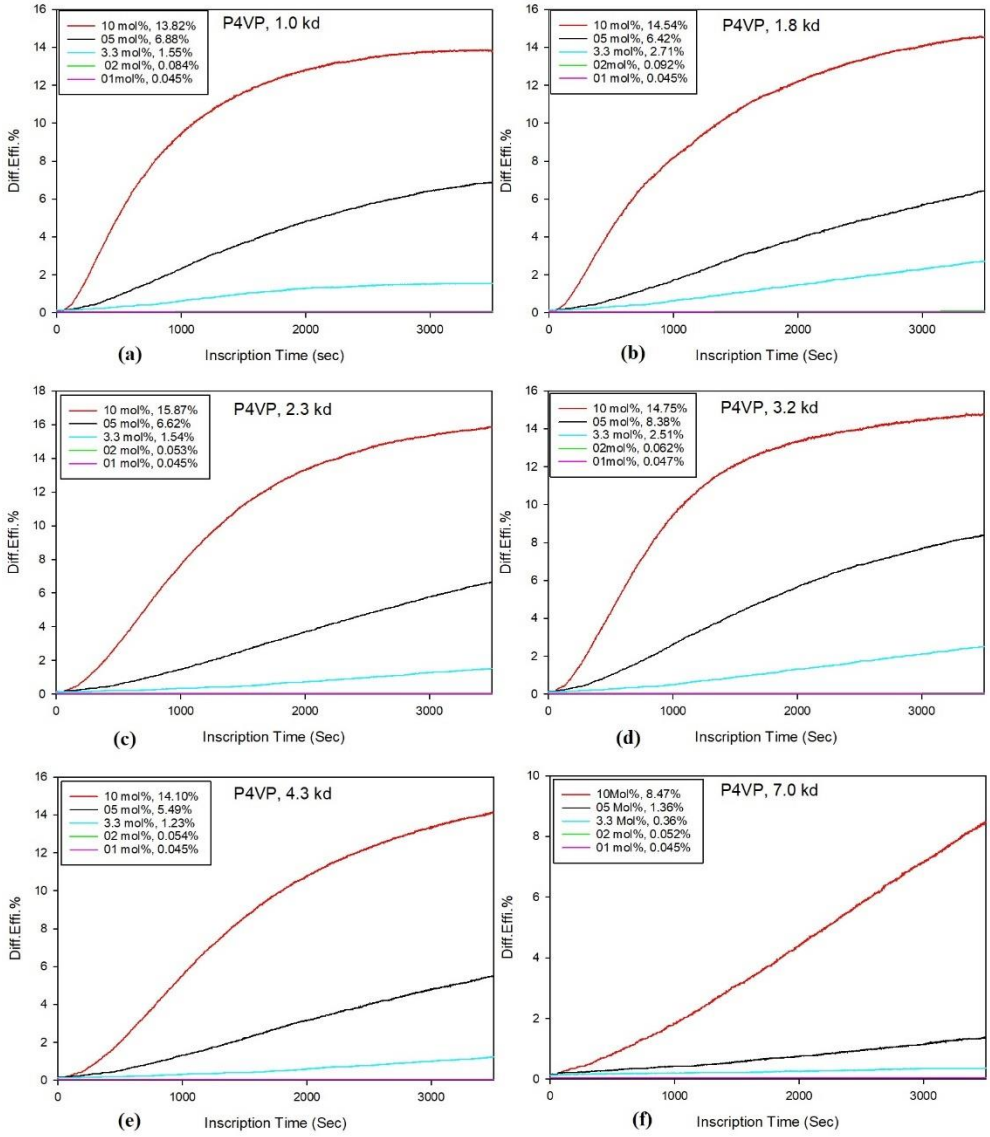

Figure 5.7: *Evolution of diffraction efficiencies for different P4VP molecular weights (a) 1kD (b) 1.8kD (c) 2.3kD (d) 3.2kD (e) 4.3kD (f) 7kD*

The systematic increase in the polymer weight as shown in Table 5.2, there is no large difference seen in the diffraction efficiencies except for the highest molecular weight (i.e. 7kD) (Figure 5.7) where the diffraction efficiency drops sufficiently with large number. In other polymeric weights the difference in the diffraction efficiency values is not of higher value. It indicates that other than the molecular weight the polymer structure and the glass transition might play an important role in the diffraction efficiency values.

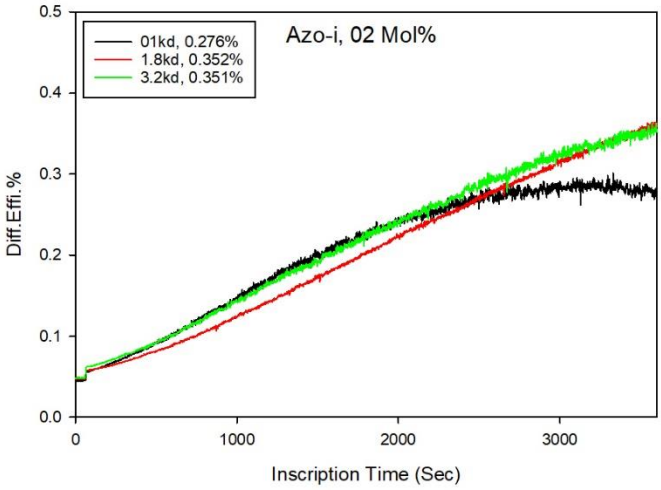

Figure 5.8: *Evolution of diffraction efficiencies for Azo-I (at X = 2 mol%)*

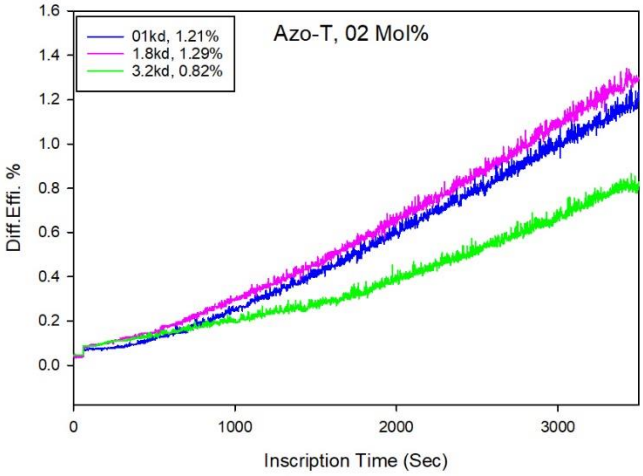

Figure 5.9: *Evolution of diffraction efficiencies for Azo-T (at X = 2 mol%)*

The halogen bond is highly directional which is caused by the narrow confinement of the electropositive bond donating region on the polarizable halogen atom [44]. The halogen bond directionality makes it useful in the designing functional supramolecular photoactive polymers [16]. In this study we study the halogen bonded polymer complexes formed with two dyes, **Azo-I** (Figure 5.8) and **Azo-T** (Figure 5.9) with different weights of polymer (P4VP). It is evident from diffraction efficiency values (Table 5.2) that **Azo-T** is more efficient relative to **Azo-I** as **Azo-T** interacts strongly with P4VP.

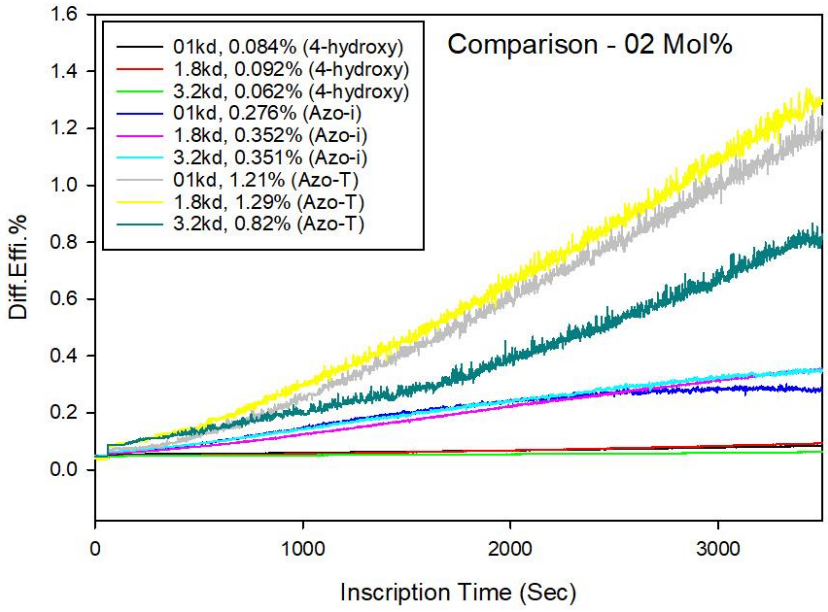

Figure 5.10: *Comparison of evolution of diffraction efficiencies, for 4-hydroxy, Azo-I and Azo-T (at X = 2mol%)*

As aforementioned that both hydrogen and halogen bonded complexes are capable of forming SRGs at the exceedingly low molecular weights (1 mol%). After establishing that, it is essential to analyze the most efficient out of these both non-covalent interactions. In this study we compare the hydrogen bonded (**4-hydroxy**) azo-polymer complex with halogen bonded (**Azo-I** and **Azo-T**) complexes in P4VP matrix at 02 mol% dye concentration for all, as shown in Figure 5.10**.** The **Azo-T** polymer complex is most efficient of all with the highest diffraction efficiency (Table 5.2) and both halogen bonded complexes are more efficient comparative to hydrogen bonded complex. We can conclude here that the halogen bonded complexes surpass the hydrogen bonded complexes and create more efficient SRGs.

6. CONCLUSIONS

In this work we studied three different azobenzene chromophores with one type of polymer matrix (P4VP), where two dyes (**Azo-I** and **Azo-T**), are halogen bonded to P4VP while **4-hydroxy** is hydrogen bonded. Two sample series of azo-polymer complexes were designed with various molar concentrations of **4-hydroxy** and molecular weights of P4VP. A series of halogen-bonded complexes was prepared at 2 mol-% concentration to compare their performance with hydrogen-bonded complexes with the same azobenzene concentration.

Surface relief grating (SRG) formation was observed in the complexes regardless of their interaction type, but with different diffraction efficiencies and requiring certain azobenzene concentration to occur. We observed that the diffraction efficiency increases with an increase in the azobenzene concentration and for higher polymer molecular weights the diffraction efficiency systematically decreases. We can conclude here that optimizing the complexation degree and the understanding the polymer structural properties can establish new facts and findings.

For halogen bonded complexes, it is evident that the **Azo-T** is more efficient compared to the other halogen-bonded azobenzene (**Azo-I**) presumably because **Azo-T** interacts more strongly with P4VP. So, it can be concluded that selection of a supramolecular interaction of sufficient strength is important. The supramolecular bond nature is even more important, since halogen bonded azobenzenes are more efficient in driving SRG formation than their hydrogen-bonded counter parts, even if hydrogen bonding is stronger than halogen bonding.

To conclude we can say that the SRG formation can be carried with low complexation degree and higher polymer molecular weights and halogen bonding surpasses the hydrogen bonding in SRG formation performance. It can be concluded also that the halogen bond effects to be stronger than the hydrogen bond at low concentrations ratios, yet further studies are needed to understand how low one can go in azobenzene concentration to still facilitate SRG formation in halogen bonded complexes.

7. REFERENCES

above

[1] A. Natansohn and P. Rochon, "Photoinduced Motions in Azo-Containing Polymers", *Chemical Reviews*, vol. 102, no. 11, pp. 4139-4176, 2002.

2] O. Lehtonen, "Comparing polymer–azobenzene complexes based on different halogen bond motifs", Bachelor's Thesis, Aalto university School of Science, Espoo, Finland, 2015.

[3] A. Priimägi, "Polymer Azobenzene Complexes: From Supramolecular Concepts to Efficient Photoresponsive Polymers", PhD Thesis, Helsinki University of Technology, Espoo, Finland, 2009.

[4] Y. Zhao and T. Ikeda, *Smart light-responsive materials*. Hoboken: A John Wiley & Sons, Inc.,Publication, 2009.

[5] T. Schultz et al., "Mechanism and Dynamics of Azobenzene Photoisomerization", *Journal of the American Chemical Society*, vol. 125, no. 27, pp. 8098-8099, 2003.

[6] L. Ding and T. Russell, "A Photoactive Polymer with Azobenzene Chromophore in the Side Chains", *Macromolecules*, vol. 40, no. 6, pp. 2267-2270, 2007.

[7] H. Bandara and S. Burdette, "Photoisomerization in different classes of azobenzene", *Chem. Soc. Rev.*, vol. 41, no. 5, pp. 1809-1825, 2012.

[8] N. Simeth, S. Crespi, M. Fagnoni and B. König, "Tuning the Thermal Isomerization of Phenylazoindole Photoswitches from Days to Nanoseconds", *Journal of the American Chemical Society*, vol. 140, no. 8, pp. 2940-2946, 2018.

[9] C. Knie et al., "ortho-Fluoroazobenzenes: Visible Light Switches with Very Long-Lived Z Isomers", *Chemistry - A European Journal*, vol. 20, no. 50, pp. 16492-16501, 2014.

[10] J. Vapaavuori, "Studies on Photoinduced Birefringence in Hydrogen-Bonded Polymer-Dye Complexes", Masters Thesis, Helsinki University of Technology, Espoo, Finland, 2008.

[11] J. Hautala, "Light-Induced Motions in Azopolymer Films doped with silver nano-particles", Masters Thesis, Aalto University School of Science, Espoo, Finland, 2014.

[12] J. Vapaavuori, R. Ras, M. Kaivola, C. Bazuin and A. Priimagi, "From partial to complete optical erasure of azobenzene–polymer gratings: effect of molecular weight", *Journal of Materials Chemistry C*, vol. 3, no. 42, pp. 11011-11016, 2015.

[13] P. Rochon, E. Batalla and A. Natansohn, "Optically induced surface gratings on azoaromatic polymer films", *Applied Physics Letters*, vol. 66, no. 2, pp. 136-138, 1995.

[14] D. Kim, S. Tripathy, L. Li and J. Kumar, "Laser-induced holographic surface relief gratings on nonlinear optical polymer films", *Applied Physics Letters*, vol. 66, no. 10, pp. 1166-1168, 1995.

[15] O. Kulikovska, L. Goldenberg and J. Stumpe, "Supramolecular Azobenzene-Based Materials for Optical Generation of Microstructures", *Chemistry of Materials*, vol. 19, no. 13, pp. 3343-3348, 2007.

[16] A. Priimagi et al., "Photoresponsive Supramolecular Polymers: Halogen Bonding versus Hydrogen Bonding in Driving Self-Assembly and Performance of Light-Responsive Supramolecular Polymers ", *Advanced Functional Materials*, vol. 22, no. 12, pp. 2571-2571, 2012.

[17] Gorynsztejn-Leben, "Photoinduced effects in Halogen Bonded and Hydrogen Bonded Polymer-Azobenzene Complexes", Diploma Thesis, Aalto University School of Science, Espoo, Finland, 2010.

[18] J. Koskela, J. Vapaavuori, R. Ras and A. Priimagi, "Light-Driven Surface Patterning of Supramolecular Polymers with Extremely Low Concentration of Photoactive Molecules", *ACS Macro Letters*, vol. 3, no. 11, pp. 1196-1200, 2014.

[19] Z. Mahimwalla, K. Yager, J. Mamiya, A. Shishido, A. Priimagi and C. Barrett, "Azobenzene photomechanics: prospects and potential applications", *Polymer Bulletin*, vol. 69, no. 8, pp. 967-1006, 2012.

[20] G. Kumar and D. Neckers, "Photochemistry of azobenzene-containing polymers", *Chemical Reviews*, vol. 89, no. 8, pp. 1915-1925, 1989.

[21] Z. Sekkat and W. Knoll, *Photoreactive organic thin films*. Amsterdam: Academic Press, 2002.

[22] G. Fou Carballond, "Photo-switchable Acids and Bases", 2008. Available at: https://www2.chemistry.msu.edu/courses/CEM958/FS08_SS09/carballo.pdf.

[23] A. Priimagi, S. Cattaneo, R. Ras, S. Valkama, O. Ikkala and M. Kauranen, "Polymer−Dye Complexes: A Facile Method for High Doping Level and Aggregation Control of Dye Molecules", *Chemistry of Materials*, vol. 17, no. 23, pp. 5798-5802, 2005.

[24] J. Gao, Y. He, F. Liu, X. Zhang, Z. Wang and X. Wang, "Azobenzene-Containing Supramolecular Side-Chain Polymer Films for Laser-Induced Surface Relief Gratings", *Chemistry of Materials*, vol. 19, no. 16, pp. 3877-3881, 2007.

[25] C. Faul and M. Antonietti, "Ionic Self-Assembly: Facile Synthesis of Supramolecular Materials", *Advanced Materials*, vol. 15, no. 9, pp. 673-683, 2003.

[26] A. Priimagi, M. Kaivola, F. Rodriguez and M. Kauranen, "Enhanced photoinduced birefringence in polymer-dye complexes: Hydrogen bonding makes a difference", *Applied Physics Letters*, vol. 90, no. 12, p. 121103, 2007.

[27] M. Saccone et al., "Supramolecular hierarchy among halogen and hydrogen bond donors in light-induced surface patterning", *Journal of Materials Chemistry C*, vol. 3, no. 4, pp. 759-768, 2015.

[28] A. Cembran, F. Bernardi, M. Garavelli, L. Gagliardi and G. Orlandi, "On the Mechanism of the cis−trans Isomerization in the Lowest Electronic States of Azobenzene: S0, S1, and T1", *Journal of the American Chemical Society*, vol. 126, no. 10, pp. 3234-3243, 2004.

[29] E. Wei-Guang Diau, "A New Trans-to-Cis Photoisomerization Mechanism of Azobenzene on the S1(n,π*) Surface", *The Journal of Physical Chemistry A*, vol. 108, no. 6, pp. 950-956, 2004.

[30] J. Delaire and K. Nakatani, "Linear and Nonlinear Optical Properties of Photochromic Molecules and Materials", *Chemical Reviews*, vol. 100, no. 5, pp. 1817-1846, 2000.

[31] T. Todorov, L. Nikolova and N. Tomova, "Polarization holography 1: A new high-efficiency organic material with reversible photoinduced birefringence", *Applied Optics*, vol. 23, no. 23, p. 4309, 1984.

[32] D. Rais, S. Nespurek, Y. Zakrevsky, J. Stump, Z. Sedlakov and M. Studenovsk, "Photo-orientation in azobenzene containing polybutadiene-based polymer", *Journal of Optoelectronics and Advanced Materials*, vol. 7, no. 3, pp. 1371-1375, 2005.

[33] H. Yu and T. Kobayashi, "Photoresponsive Block Copolymers Containing Azobenzenes and Other Chromophores", *Molecules*, vol. 15, no. 1, pp. 570-603, 2010.

[34] E. Hecht, *Optics*, 4th ed. London, United Kingdom: Pearson Publishing Company, 2002.

[35] R. Hagen and T. Bieringer, "Photoaddressable Polymers for Optical Data Storage", *Advanced Materials*, vol. 13, no. 23, pp. 1805-1810, 2001.

[36] S. Hvilsted, F. Andruzzi and P. Ramanujam, "Side-chain liquid-crystalline polyesters for optical information storage", *Optics Letters*, vol. 17, no. 17, p. 1234, 1992.

[37] A. Priimagi and A. Shevchenko, "Azopolymer-based micro- and nanopatterning for photonic applications", *Journal of Polymer Science Part B: Polymer Physics*, vol. 52, no. 3, pp. 163-182, 2013.

[38] A. Priimagi, K. Lindfors, M. Kaivola and P. Rochon, "Efficient Surface-Relief Gratings in Hydrogen-Bonded Polymer−Azobenzene Complexes", *ACS Applied Materials & Interfaces*, vol. 1, no. 6, pp. 1183-1189, 2009.

[39] H. Lodish, *Molecular cell biology*. New York: W.H. Freeman, 2000.

[40] V. Kannan, "Non-covalent bonds", *Slideshare.net*, 2015. Available at: https://www.slideshare.net/VipinKannan1/non-covalent-bonds.

[41] C. Robertson, J. Wright, E. Carrington, R. Perutz, C. Hunter and L. Brammer, "Hydrogen bonding vs. halogen bonding: the solvent decides", *Chemical Science*, vol. 8, no. 8, pp. 5392-5398, 2017.

[42] W. Masterton, *Principles of Organic Synthesis, 3rd Edition*, 3rd ed. Massachusetts: Harcourt College Publishers, 1996, pp. 240-244.

[43] E. Arunan et al., "Definition of the hydrogen bond (IUPAC Recommendations 2011)", *Pure and Applied Chemistry*, vol. 83, no. 8, pp. 1637-1641, 2011.

[44] J. Vapaavuori, C. Bazuin and A. Priimagi, "Supramolecular design principles for efficient photoresponsive polymer–azobenzene complexes", *Journal of Materials Chemistry C*, vol. 6, no. 9, pp. 2168-2188, 2018.

[45] T. Seki, T. Fukuchi and K. Ichimura, "Role of Hydrogen Bonding in Azobenzene−Urea Assemblies. The Packing State and Photoresponse Behavior in Langmuir Monolayers", *Langmuir*, vol. 18, no. 14, pp. 5462-5467, 2002.

[46] G. Desiraju et al., "Definition of the halogen bond (IUPAC Recommendations 2013)", *Pure and Applied Chemistry*, vol. 85, no. 8, pp. 1711-1713, 2013.

[47] A. Priimagi, G. Cavallo, P. Metrangolo and G. Resnati, "The Halogen Bond in the Design of Functional Supramolecular Materials: Recent Advances", *Accounts of Chemical Research*, vol. 46, no. 11, pp. 2686-2695, 2013.

[48] G. Cavallo et al., "The Halogen Bond", *Chemical Reviews*, vol. 116, no. 4, pp. 2478-2601, 2016.

[49] A. Barroso, "Development of Advanced interferometric techniques for the study of cell-material interaction", PhD Thesis, University of Naples, Italy, 2016.

[50] J. Vapaavuori et al., "Photomechanical Energy Transfer to Photopassive Polymers through Hydrogen and Halogen Bonds", *Macromolecules*, vol. 48, no. 20, pp. 7535-7542, 2015.